9

Frequency Stability and Control

Previous chapters have described how the generators in a power system respond when there is a momentary disturbance in the power balance between the electrical power consumed in the system and the mechanical power delivered by the turbines. Such disturbances are caused by short circuits in the transmission network and are normally cleared without the need to reduce the generated or consumed power. However, if a large load is suddenly connected (or disconnected) to the system, or if a generating unit is suddenly disconnected by the protection equipment, there will be a long-term distortion in the power balance between that delivered by the turbines and that consumed by the loads. This imbalance is initially covered from the kinetic energy of rotating rotors of turbines, generators and motors and, as a result, the frequency in the system will change. This frequency change can be conveniently divided into a number of stages allowing the dynamics associated with each of these stages to be described separately. This helps illustrate how the different dynamics develop in the system. However, it is first necessary to describe the operation of the automatic generation control (AGC) as this is fundamental in determining the way in which the frequency will change in response to a change in load.

扭曲, 失真

The general framework of frequency control described in this chapter was originally developed under the framework of traditional vertically integrated utilities which used to control generation, transmission and often distribution in their own service areas and where power interchanges between control areas were scheduled in advance and strictly adhered to. Chapter 2 described liberalization of the industry taking place in many countries in the world since the 1990s whereby utilities are no longer vertically integrated generation companies that compete against each other and the coordination necessary for reliable system operation, including frequency control, is undertaken by Transmission System Operators (TSOs). The framework of frequency control had to be adapted to the market environment in the sense that TSOs have to procure, and pay for, frequency support from individual power plants. The way those services are procured differs from country to country so the commercial arrangements will not be discussed in this book. However, the overall hierarchical control framework has been largely retained, with only some changes in the tertiary control level, as discussed later in this chapter.

The discussion will concentrate on frequency control in an interconnected power system, using the European UCTE as the example. It is worth adding that the framework of frequency control in an islanded system, such as in the United Kingdom, may be different. Also, the meaning of some of the terms may differ from country to country.

Power System Dynamics: Stability and Control, Second Edition Jan Machowski, Janusz W. Bialek and James R. Bumby

9.1 Automatic Generation Control 自动发电控制

Section 2.1 explained how an electrical power system consists of many generating units and many loads while its total power demand varies continuously throughout the day in a more or less anticipated manner. The large, slow changes in demand are met centrally by deciding at regular intervals which generating units will be operating, shut down or in an intermediate hot reserve state. This process of *unit commitment* may be conducted once per day to give the daily operating schedule, while at shorter intervals, typically every 30 min, *economic dispatch* determines the actual power output required from each of the committed generators. Smaller, but faster, load changes are dealt with by AGC so as to:

- maintain frequency at the scheduled value (frequency control);
- maintain the net power interchanges with neighbouring control areas at their scheduled values (tie-line control);
- maintain power allocation among the units in accordance with area dispatching needs (energy market, security or emergency).

In some systems the role of AGC may be restricted to one or two of the above objectives. For example, tie-line power control is only used where a number of separate power systems are interconnected and operate under mutually beneficial contractual agreements.

9.1.1 Generation Characteristic

Section 2.2.3 discussed the operation of turbines and their governing systems. In the steady state the idealized power–speed characteristic of a single generating unit is given by Equation (2.3). As the rotational speed is proportional to frequency, Equation (2.3) may be rewritten for the ith generating unit as

$$\frac{\Delta f}{f_{\mathrm{n}}} = -\rho_i \frac{\Delta P_{\mathrm{m}i}}{P_{\mathrm{n}i}}, \quad \frac{\Delta P_{\mathrm{m}i}}{P_{\mathrm{n}i}} = -K_i \frac{\Delta f}{f_{\mathrm{n}}}. \tag{9.1}$$

In the steady state all the generating units operate synchronously at the same frequency when the overall change in the total power ΔP_{T} generated in the system can be calculated as the sum of changes at all generators:

$$\Delta P_{\mathrm{T}} = \sum_{i=1}^{N_{\mathrm{G}}} \Delta P_{\mathrm{m}i} = -\frac{\Delta f}{f_{\mathrm{n}}} \sum_{i=1}^{N_{\mathrm{G}}} K_i P_{\mathrm{n}i} = -\Delta f \sum_{i=1}^{N_{\mathrm{G}}} \frac{K_i P_{\mathrm{n}i}}{f_{\mathrm{n}}}, \tag{9.2}$$

where N_{G} is the number of generating units in the system. The subscript 'T' indicates that ΔP_{T} is the change in generated power as supplied by the turbines. Figure 9.1 illustrates how the characteristics of individual generating units can be added according to Equation (9.2) to obtain the equivalent

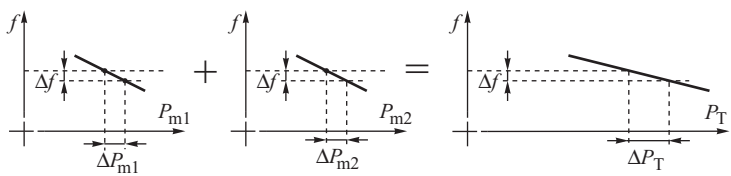

Figure 9.1 Generation characteristic as the sum of the speed–droop characteristics of all the generation units.

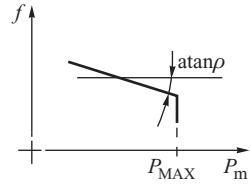

Figure 9.2 Speed–droop characteristic of a turbine with an upper limit.

generation characteristic. This characteristic defines the ability of the system to compensate for a power imbalance at the cost of a deviation in frequency. For a power system with a large number of generating units, the generation characteristic is almost horizontal such that even a relatively large power change only results in a very small frequency deviation. This is one of the benefits accruing from combining generating units into one large system.

To obtain the equivalent generation characteristic of Figure 9.1 it has been assumed that the speed–droop characteristics of the individual turbine generator units are linear over the full range of power and frequency variations. In practice the output power of each turbine is limited by its technical parameters. For example, coal-burn steam turbines have a lower power limit due to the need to maintain operational stability of the burners and an upper power limit that is set by thermal and mechanical considerations. In the remainder of this section only the upper limit will be considered, so the turbine characteristic will be as shown in Figure 9.2.

If a turbine is operating at its upper power limit then a decrease in the system frequency will not produce a corresponding increase in its power output. At the limit $\rho = \infty$ or $K = 0$ and the turbine does not contribute to the equivalent system characteristic. Consequently the generation characteristic of the system will be dependent on the number of units operating away from their limit at part load; that is, it will depend on the *spinning reserve*, where the spinning reserve is the difference between the sum of the power ratings of all the operating units and their actual load. The allocation of spinning reserve is an important factor in power system operation as it determines the shape of the generation characteristic. This is demonstrated in Figure 9.3 which shows a simple case of two generating units. In Figure 9.3a the spinning reserve is allocated proportionally to both units so that they both reach their upper power limits at the same frequency f_1. In this case the equivalent characteristic, obtained from Equation (9.2), is linear until the upper power limit for the whole system is reached. In Figure 9.3b the same amount of spinning reserve is available but is allocated solely to the second generator with the first unit operating at full load. The generation characteristic is now nonlinear and consists of two sections of different slope.

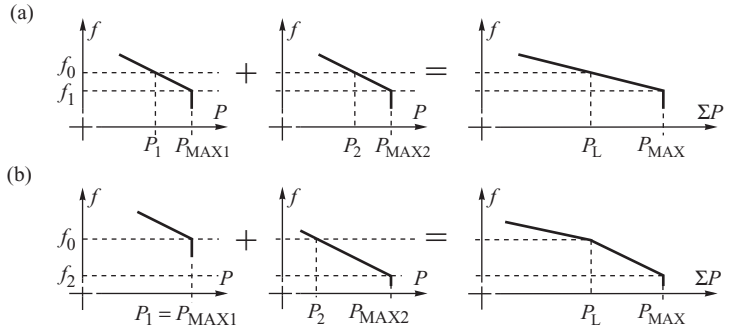

Figure 9.3 Influence of the turbine upper power limit and the spinning reserve allocation on the generation characteristic.

Similarly, the generation characteristic of an actual power system is nonlinear and consists of many short sections of increasing slope as more and more generating units reach their operating limits as the total load increases until, at maximum system load, there is no more spinning reserve available. The generation characteristic then becomes a vertical line. For small power and frequency disturbances it is convenient to approximate this nonlinear generation characteristic in the vicinity of the operation point by a linear characteristic with a local droop value. The total system generation is equal to the total system load P_{L} (including transmission losses)

$$\sum_{i=1}^{N_{\mathrm{G}}} P_{\mathrm{m}i} = P_{\mathrm{L}}, \tag{9.3}$$

where N_{G} is the number of generating units. Dividing Equation (9.2) by P_{L} gives

$$\frac{\Delta P_{\mathrm{T}}}{P_{\mathrm{L}}} = -K_{\mathrm{T}} \frac{\Delta f}{f_{\mathrm{n}}} \quad \text{or} \quad \frac{\Delta f}{f_{\mathrm{n}}} = -\rho_{\mathrm{T}} \frac{\Delta P_{\mathrm{T}}}{P_{\mathrm{L}}}, \tag{9.4}$$

where

$$K_{\mathrm{T}} = \frac{\sum_{i=1}^{N_{\mathrm{G}}} K_i P_{\mathrm{n}i}}{P_{\mathrm{L}}}, \quad \rho_{\mathrm{T}} = \frac{1}{K_{\mathrm{T}}}. \tag{9.5}$$

Equation (9.4) describes the linear approximation of the generation characteristic calculated for a given total system demand. Consequently, the coefficients in Equation (9.5) are calculated with respect to the total demand, not the sum of the power ratings, so that ρ_{T} is the local speed droop of the generation characteristic and depends on the spinning reserve and its allocation in the system as shown in Figure 9.3.

In the first case, shown in Figure 9.3a, it was assumed that the spinning reserve is allocated uniformly between both generators, that is both generators are underloaded by the same amount at the operating point (frequency f_0) and the maximum power of both generators is reached at the same point (frequency f_1). The sum of both characteristics is then a straight line up to the maximum power $P_{\mathrm{MAX}} = P_{\mathrm{MAX}1} + P_{\mathrm{MAX}2}$. In the second case, shown in Figure 9.3b, the total system reserve is the same but it is allocated to the second generator only. That generator is loaded up to its maximum at the operating point (frequency f_2). The resulting total generation characteristic is nonlinear and consists of two lines of different slope. The first line is formed by adding both inverse droops, $K_{\mathrm{T}1} \neq 0$ and $K_{\mathrm{T}2} \neq 0$, in Equation (9.5). The second line is formed noting that the first generator operates at maximum load and $K_{\mathrm{T}1} = 0$ so that only $K_{\mathrm{T}2} \neq 0$ appears in the sum in Equation (9.5). Hence the slope of that characteristic is higher.

The number of units operating in a real system is large. Some of them are loaded to the maximum but others are partly loaded, generally in a non-uniform way, to maintain a spinning reserve. Adding up all the individual characteristics would give a nonlinear resulting characteristic consisting of short segments with increasingly steeper slopes. That characteristic can be approximated by a curve shown in Figure 9.4. The higher the system load, the higher the droop until it becomes infinite $\rho_{\mathrm{T}} = \infty$, and its inverse $K_{\mathrm{T}} = 0$, when the maximum power P_{MAX} is reached. If the dependence of a power station's auxiliary requirements on frequency were neglected, that part of the characteristic would be vertical (shown as a dashed line in Figure 9.4). However, power stations tends to have a curled-back characteristic – see curve 4 in Figure 2.13. Similarly curled is the system characteristic shown in Figure 9.4.

For further considerations, the nonlinear generation characteristic shown in Figure 9.4 will be linearized at a given operating point, that is the linear approximation (9.4) will be assumed with the droop ρ_{T} given by (9.5).

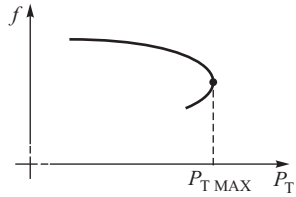

Figure 9.4 Static system generation characteristic.

9.1.2 Primary Control

When the total generation is equal to the total system demand (including losses) then the frequency is constant, the system is in equilibrium, and the generation characteristic is approximated by Equation (9.4). However, as discussed in Section 3.5, system loads are also frequency dependent and an expression similar to Equation (9.4) can be used to obtain a linear approximation of the frequency response characteristic of the total system load as

$$\frac{\Delta P_L}{P_L} = K_L \frac{\Delta f}{f_n}, \tag{9.6}$$

where K_L is the *frequency sensitivity coefficient of the power demand*. A similar coefficient k_{Pf} was defined in Equation (3.133) and referred to as the frequency sensitivity of a single composite load and should not be confused with K_L above, which relates to the total system demand. Tests conducted on actual systems indicate that the generation response characteristic is much more frequency dependent than the demand response characteristic. Typically K_L is between 0.5 and 3 (see Table 3.3) while $K_T \approx 20$ ($\rho = 0.05$). In Equations (9.4) and (9.6) the coefficients K_T and K_L have opposite sign so that an increase in frequency corresponds to a drop in generation and an increase in electrical load.

In the (P, f) plane the intersection of the generation and the load characteristic, Equations (9.4) and (9.6), defines the system equilibrium point. A change in the total power demand ΔP_L corresponds to a shift of the load characteristic in the way shown in Figure 9.5 so that the equilibrium point is moved from point 1 to point 2. The increase in the system load is compensated in two ways: firstly, by the turbines increasing the generation by ΔP_T; and secondly, by the system loads reducing the demand by ΔP_L from that required at point 3 to that required at point 2. Figure 9.5 shows that taking both increments into account gives

$$\Delta P_{demand} = \Delta P_T - \Delta P_L = -(K_T + K_L) P_L \frac{\Delta f}{f_n} = -K_f P_L \frac{\Delta f}{f_n}. \tag{9.7}$$

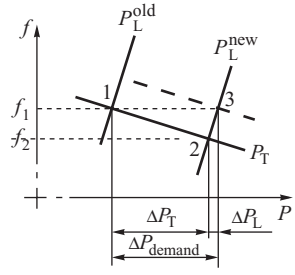

Figure 9.5 Equilibrium points for an increase in the power demand.

The new operating point of the system corresponds to a new demand and a new frequency. The new value of the system frequency f_2 is lower than the old one f_1. Equation (9.7) represents the frequency response of the system while the coefficient $K_f = K_T + K_L$ is referred to as the *stiffness*. It should be emphasized that $\Delta P_T \gg \Delta P_L$.

A reduction of the demand by ΔP_L is due to the frequency sensitivity of demand. An increase of generation by ΔP_T is due to turbine governors. The action of turbine governors due to frequency changes when reference values of regulators are kept constant is referred to as *primary frequency control*.

When the system demand increases, primary control is activated, obviously only if there are any units which are operating but are not fully loaded. Figure 9.3b shows that if any of the units operate at maximum output, a reduction in frequency cannot increase a unit's output. Only those units that are partly loaded and carry a spinning reserve can be loaded more.

In order to secure safe system operation and a possibility of activating the primary control, the system operator must have an adequate spinning reserve at its disposal. Spinning reserve to be utilized by the primary control should be uniformly distributed around the system, that is at power stations evenly located around the system. Then the reserve will come from a variety of locations and the risk of overloading some transmission corridors will be minimized. Locating the spinning reserve in one region may be dangerous from the point of view of security of the transmission network. If one or more power stations suffer outages, the missing power would come from just one region, some transmission corridors might get overloaded and the disturbance might spread.

An interconnected system requires coordination so the requirements regarding the primary control are normally the subject of agreements between partners cooperating in a given interconnected network. For the European UCTE system, the requirements are defined in document 'UCTE – Ground Rules – Supervision of the application of rules concerning primary and secondary control of frequency and active power in UCTE'.

For the purposes of primary frequency control, each subsystem in the UCTE system has to ensure a large enough spinning reserve proportional to a given subsystem's share in the overall UCTE energy production. This is referred to as the *solidarity principle*. It is required that the spinning reserve is uniformly located within each subsystem and the operating points of individual units providing the reserve are such that the whole reserve in the system is activated when the frequency deviation is not more than 200 mHz. The required time of activation of the reserve

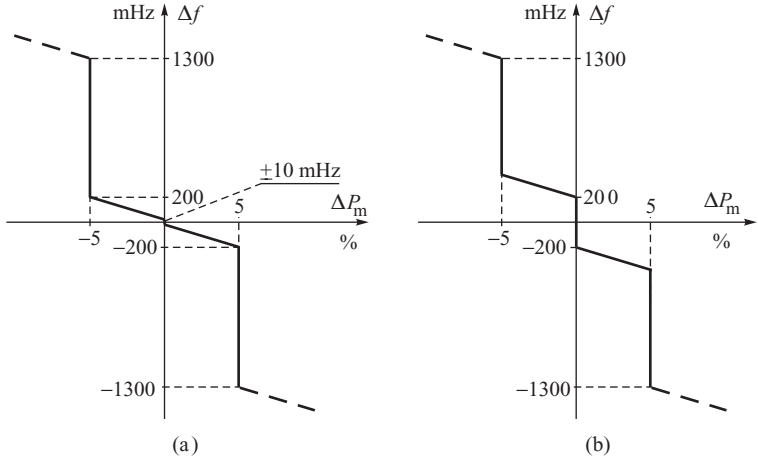

Figure 9.6 Example of speed – droop characteristics: (a) with small dead zones; (b) with large dead zones.

should not be longer than 15–23 s. To satisfy this condition, the units participating in the primary reserve should be able to regulate power quickly within ±5 % of their rated power. Turbine governors of those units have typically speed–droop characteristics with dead zones as in Figure 9.6a. The first dead zone has the width ±10 mHz which makes the unit operate with constant set power P_{ref} in the presence of small frequency error $|\Delta f| < 10$ mHz . When a frequency error $|\Delta f| > 10$ mHz appears, the unit operates in the primary control with a fast regulation range ±5 %. The whole range of the reserve is released when the frequency error is about ±200 mHz. These requirements mean the whole primary reserve is released in the system when the frequency error is not greater than 200 mHz. The droop can be calculated in the fast regulation range from (9.1). Substituting $\Delta f = (200 - 10)$ mHz $= 190$ mHz $= 0.190$ Hz , that is $\Delta f / f_{\text{n}} = 0.190/50 = 0.0038$ and $\Delta P_{\text{m}} / P_{\text{n}} = -0.05$, results in $\rho = 0.0038/0.05 = 0.076 = 7.6\,\%$. This is a typical value as, according to Section 2.2.3, the droop ρ is typically assumed to be between 4 and 9 %. For the range beyond fast regulation ±5 % the turbine governor maintains constant power until the frequency error reaches $|\Delta f| > 1300$ mHz $= 1.3$ Hz when the governor is switched from the power control regime to speed control.

Governors of units that do not participate in the primary frequency control have the first dead zone of the speed – droop characteristic set at ±200 mHz (Figure 9.6b). They form an additional primary reserve that activates only for large disturbances. This is necessary to defend the system against blackouts (details in Section 9.1.6).

9.1.3 Secondary Control

If the turbine–generators (涡轮发电机) are equipped with governing systems, such as those described in Section 2.2.3, then, following a change in the total power demand, the system will not be able to return to the initial frequency on its own, without any additional action. According to Figure 9.5, in order to return to the initial frequency the generation characteristic must be shifted to the position shown by the dashed line. Such a shift can be enforced by changing the P_{ref} setting in the turbine governing system (the load reference set point in Figure 2.14). As shown in Figure 9.7, changes in the settings $P_{\text{ref(1)}}$, $P_{\text{ref(2)}}$ and $P_{\text{ref(3)}}$ enforce a corresponding shift of the characteristic to the positions $P_{\text{m(1)}}$, $P_{\text{m(2)}}$ and $P_{\text{m(3)}}$. To simplify, the first dead zone around P_{ref}, which was shown in Figure 9.6, has been neglected in Figure 9.7. Obviously no change of settings can force a turbine to exceed its maximum power rating P_{MAX}. Changing more settings P_{ref} of individual governors will move upwards the overall generation characteristic of the system. Eventually this will lead to the restoration of the rated frequency but now at the required increased value of power demand. Such control action on the governing systems of individual turbines is referred to as *secondary control*.

In an isolated power system, automatic secondary control may be implemented as a decentralized control function by adding a supplementary control loop to the turbine–governor system. This modifies the block diagram of the turbine governor, Figure 2.14, to that shown in Figure 9.8 where P_{ref} and P_{m} are expressed as a fraction of the rated power P_{n}. The supplementary control loop,

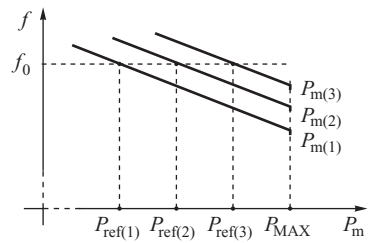

Figure 9.7 Turbine speed–droop characteristics for various settings of P_{ref}.

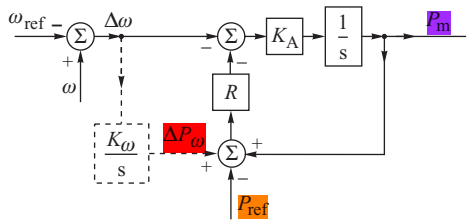

Figure 9.8 Supplementary control added to the turbine governing system.

shown by the dashed line, consists of an integrating element which adds a control signal ΔP_ω that is proportional to the integral of the speed (or frequency) error to the load reference point. This signal modifies the value of the setting in the P_{ref} circuit thereby shifting the speed–droop characteristic in the way shown in Figure 9.7.

Not all the generating units in a system that implements decentralized control need be equipped with supplementary loops and participate in secondary control. Usually medium-sized units are used for frequency regulation while large base load units are independent and set to operate at a prescribed generation level. In combined cycle gas and steam turbine power plants the supplementary control may affect only the gas turbine or both the steam and the gas turbines.

In an interconnected power system consisting of a number of different control areas, secondary control cannot be decentralized because the supplementary control loops have no information as to where the power imbalance occurs so that a change in the power demand in one area would result in regulator action in all the other areas. Such decentralized control action would cause undesirable changes in the power flows in the tie-lines linking the systems and the consequent violation of the contracts between the cooperating systems. To avoid this, centralized secondary control is used.

In interconnected power systems, AGC is implemented in such a way that each area, or subsystem, has its own central regulator. As shown in Figure 9.9, the power system is in equilibrium if, for each area, the total power generation P_{T}, the total power demand P_{L} and the net tie-line interchange power P_{tie} satisfy the condition

$$P_{\text{T}} - (P_{\text{L}} + P_{\text{tie}}) = 0. \tag{9.8}$$

The objective of each area regulator is to maintain frequency at the scheduled level (frequency control) and to maintain net tie-line interchanges from the given area at the scheduled values (tie-line control). If there is a large power balance disturbance in one subsystem (caused for example by the tripping of a generating unit), then regulators in each area should try to restore the frequency and net tie-line interchanges. This is achieved when the regulator in the area where the imbalance originated enforces an increase in generation equal to the power deficit. In other words, each area regulator should enforce an increased generation covering its own area power imbalance and maintain planned net tie-line interchanges. This is referred to as the *non-intervention rule*.

发生不平衡的区域中的调节器强制增加与发电量相等的发电

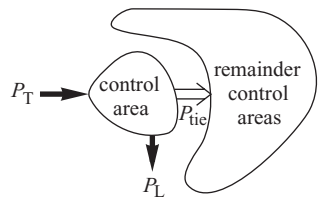

Figure 9.9 Power balance of a control area.

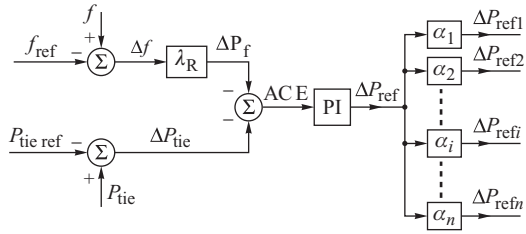

Figure 9.10 Functional diagram of a central regulator.

The regulation is executed by changing the power output of turbines in the area through varying P_{ref} in their governing systems. Figure 9.10 shows a functional diagram of the central regulator. Frequency is measured in the local low-voltage network and compared with the reference frequency to produce a signal that is proportional to the frequency deviation Δf. The information on power flows in the tie-lines is sent via telecommunication lines to the central regulator which compares it with the reference value in order to produce a signal proportional to the tie-line interchange error ΔP_{tie}. Before adding these two signals together, the frequency deviation is amplified by the factor λ_{R}, called the *frequency bias factor*, to obtain

$$\Delta P_{\text{f}} = \lambda_{\text{R}} \Delta f. \tag{9.9}$$

Amplified frequency deviation = frequency bias factor * frequency deviation

This represents a change in the generation power which must be forced upon the controlled area in order to compensate for the frequency deviation resulting from the power imbalance in this area.

The choice of the bias factor λ_{R} plays an important role in the non-intervention rule. According to this rule, each subsystem should cover its own power imbalance and try to maintain planned power interchanges. If the frequency drops following a generation deficit, then applying (9.7) gives $\Delta P_{\text{demand}} = -(K_{\text{f}} P_{\text{L}}/f_{\text{n}})\,\Delta f$. The central regulator should enforce an increased generation $\Delta P_{\text{f}} = \lambda_{\text{R}} \Delta f$ covering the deficit, that is $\Delta P_{\text{f}} = -\Delta P_{\text{demand}}$. Hence $\lambda_{\text{R}} \Delta f = (K_{\text{f}} P_{\text{L}}/f_{\text{n}})\,\Delta f$ or

$$\lambda_{\text{R}} = \frac{K_{\text{f}} P_{\text{L}}}{f_{\text{n}}} = K_{\text{f MW/Hz}}. \tag{9.10}$$

This equation indicates that the value of the bias λ_{R} can be assessed providing that the stiffness K_{f} of a given area and its total demand are known. $K_{\text{f MW/Hz}}$ denotes the frequency stiffness of the power system expressed in MW/Hz.

Clearly the non-intervention rule requires that the value of the bias set in the central regulator is equal to the area stiffness expressed in MW/Hz. In practice it is difficult to evaluate the exact value of the stiffness so that imprecise setting of the bias λ_{R} in the central regulator may have some undesirable effects on the regulation process. This will be discussed later in this chapter.

The signal ΔP_{f} is added to the net tie-line interchange error ΔP_{tie} so that the *area control error* (ACE) is created:

$$\text{ACE} = -\Delta P_{\text{tie}} - \lambda_{\text{R}} \Delta f. \tag{9.11}$$

Similarly, as in the decentralized regulator shown in Figure 9.8, the central regulator must have an integrating element in order to remove any error and this may be supplemented by a proportional element. For such a PI regulator the output signal is

$$\Delta P_{\text{ref}} = \beta_{\text{R}}(\text{ACE}) + \frac{1}{T_{\text{R}}} \int_0^t (\text{ACE})\, \text{d}t, \tag{9.12}$$

where β_R and T_R are the regulator parameters. Usually a regulator with a small, or even zero, participation of the proportional element is used, that is an integral element.

ACE corresponds to the power by which the total area power generation must be changed in order to maintain both the frequency and the tie-line flows at their scheduled values. The regulator output signal ΔP_{ref} is then multiplied by the *participation factors* $\alpha_1, \alpha_2, \ldots, \alpha_n$ which define the contribution of the individual generating units to the total generation control, Figure 9.10. The control signals $\Delta P_{ref1}, \Delta P_{ref2}, \ldots, \Delta P_{refn}$ obtained in this way are then transmitted to the power plants and delivered to the reference set points of the turbine governing systems (Figure 2.11). As with decentralized control, not all generating units need participate in generation control.

It is worth noting that regulation based on ACE defined by (9.11) does not always finish with the removal of both errors Δf and ΔP_{tie}. According to (9.11), zeroing of ACE can be generally achieved in two ways:

1. Zeroing of both errors, that is achieving $\Delta P_{tie} = 0$ and $\Delta f = 0$. This is a more desirable outcome. When the available regulation power in a given subsystem is large enough to cover its own power deficit, then the non-intervention rule enforces a return of the interchange power to a reference value and both frequency and power interchange errors are removed.
2. Achieving a compromise between the errors $\Delta P_{tie} + \lambda_R \Delta f = 0$ or $\Delta P_{tie} = -\lambda_R \Delta f$. When all the available regulation power in a given subsystem is not large enough to cover its own power imbalance, then the regulating units in that subsystem exhaust their capability before the errors are removed and the regulation ends with the violation of a reference value of power interchange. The missing power must be delivered from neighbouring networks. In that case the non-intervention rule will be violated and the following errors arise: $\Delta P_{tie\infty} = -\lambda_R \Delta f_\infty$, where $\Delta P_{W\infty}$ is power which the subsystem must additionally import to cover the power deficit.

Both cases will be illustrated in Section 9.2 using the results of computer simulation.

The exact determination of the actual stiffness $K_{fMW/Hz}$ in real time is a difficult task as the stiffness is continuously varying due to changes in the demand, its structure and the composition of power stations. Determination of $K_{fMW/Hz}$ in real time is the subject of on-going research. Generally, it would require a sophisticated dynamic identification methodology. In practice, the frequency bias factors λ_R are set in central regulators in the European UCTE system using a simplified methodology. In each year, the share of a given control area in the total energy production is determined. Then the value of $K_{fMW/Hz}$ is estimated for the whole interconnected system. This estimate of $K_{fMW/Hz}$ is divided between the control areas in proportion to their annual energy share and that value is set to be the frequency bias factor for each area.

For example, let $K_{fMW/Hz} = 20\,000$ MW/Hz be the estimate of stiffness of the whole interconnected system. Let the shares of the kth and jth control areas in the annual energy production be respectively $\alpha_k = 0.05$ and $\alpha_j = 0.20$. According to the approximate method, the frequency bias factors set in the central regulators are

$$\lambda_{Rk} = \alpha_k K_{f\,MW/Hz} = 0.05 \cdot 20\,000 = \overset{10000}{\cancel{1000}}\ \text{MW/Hz}$$

$$\lambda_{Rj} = \alpha_j K_{f\,MW/Hz} = 0.02 \cdot 20\,000 = 4000\ \text{MW/Hz}.$$

The described method is simple and results in an approximate fulfilment of the non-intervention rule.

Secondary frequency control is much slower than the primary one. As an example, given below is a description of requirements agreed by members of the European UCTE system.

Tie-line flow measurements have to be sent to the central regulator either cyclically or whenever the flow exceeds a certain value, with a delay not exceeding 1–5 s. Instructions to change the reference values are sent from the central regulator (Figure 9.10) to area regulators approximately

every 10 min. For the maximum speed of secondary control, activation of the whole range of secondary reserve must be done within 15 min.

Power stations contributing to secondary control, that is those controlled by the central regulator, must operate with a wide range of power regulation. This range depends on the type of the power station. For thermal plants, the typical range of power regulation operated within primary control (Figure 2.13) is from 40 % (technical minimum) to 100 % (maximum). Usually secondary control uses about ±5 % of the maximum power from within that range. The speed of regulation depends on the type of a unit. It is required that the speed of regulation is not less than:

- for gas or oil units: 8 % of rated power per minute;
- for coal and lignite units: 2–4 % of rated power per minute;
- for nuclear units: 1–5 % of rated power per minute;
- for hydro units: 30 % of rated power per minute.

The sum of regulation ranges, up and down, of all the generating units active in secondary control is referred to as the *bandwidth of secondary control*. The positive value of the bandwidth, that is from the maximum to the actual operating point, forms the *reserve of secondary control*. In the European UCTE system, the required value of the secondary reserve for each control area is in the range of 1 % of the power generated in the area. It is additionally required that the secondary reserve is equal at least to the size of the largest unit operating in the area. This requirement is due to the non-intervention rule if the largest unit is suddenly lost. If that happens, secondary control in the area must quickly, in no longer than 15 min, increase the power generated in the area by the value of the lost power.

The schedule of required values of power interchange $P_{\text{tie ref}}$ is sent to the central regulator based on a schedule for the whole interconnection. In order to prevent power swings between control areas due to rapid changes in the reference values, changes in the values of $P_{\text{tie ref}}$ are phased in as shown in Figure 9.11. The ramp of phasing in starts 5 min before, and finishes 5 min after, the set time of the change.

9.1.4 Tertiary Control

Tertiary control is additional to, and slower than, primary and secondary frequency control. The task of tertiary control depends on the organizational structure of a given power system and the role that power plants play in this structure.

Under the vertically integrated industry structure (see Chapter 2), the system operator sets the operating points of individual power plants based on the economic dispatch, or more generally optimal power flow (OPF), which minimizes the overall cost of operating plants subject to network constraints. Hence tertiary control sets the reference values of power in individual generating units to the values calculated by optimal dispatch in such a way that the overall demand is satisfied together with the schedule of power interchanges.

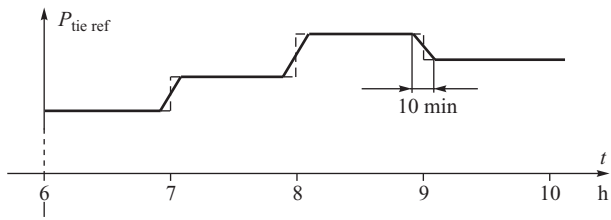

Figure 9.11 A schedule of changes in the required value of power interchange.

In many parts of the world, electricity supply systems have been liberalized and privately owned power plants are not directly controlled by the system operator. Economic dispatch is then executed via an energy market. Depending on the actual market structure in place, power plants either bid their prices to a centralized pool or arrange bilateral contracts directly with companies supplying power to individual customers. The main task of the system operator is then to adjust the supplied bids or contracts to make sure that the network constraints are satisfied and to procure the required amount of primary and secondary reserve from individual power plants. In such a market structure the task of tertiary control is to adjust, manually or automatically, the set points of individual turbine governors in order to ensure the following:

1. Adequate spinning reserve in the units participating in primary control.
2. Optimal dispatch of units participating in secondary control.
3. Restoration of the bandwidth of secondary control in a given cycle.

Tertiary control is supervisory with respect to the secondary control that corrects the loading of individual units within an area. Tertiary control is executed via the following:

1. Automatic change of the reference value of the generated power in individual units.
2. Automatic or manual connection or disconnection of units that are on the reserve of the tertiary control.

The reserve of the tertiary control is made up of those units that can be manually or automatically connected within 15 min of a request being made. The reserve should be utilized in such a way that the bandwidth of the secondary control is restored.

9.1.5 AGC as a Multi-Level Control

AGC is an excellent example of a multi-level control system whose overall structure is shown in Figure 9.12.

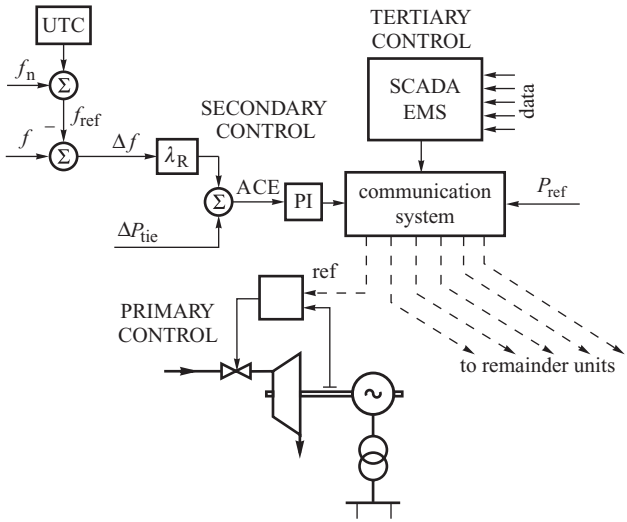

Figure 9.12 Levels of automatic generation control.

The turbine governing system with its load reference point is at the lowest primary control level and all the commands from the upper levels are executed at this level. Primary control is decentralized because it is installed in power plants situated at different geographical sites.

Frequency control and tie-line control constitute secondary control and force primary control to eliminate the frequency and net tie-line interchange deviations. In isolated systems secondary control is limited to frequency control and could be implemented locally without the need for coordination by the central regulator. In interconnected systems secondary control of frequency and tie-line flows is implemented using a central computer. Secondary control should be slower than primary control.

The task of tertiary control is to ensure an appropriate bandwidth of secondary control. Obviously tertiary control must be slower than both primary and secondary control. Hence it may be neglected when considering the dynamics of coordination between primary and secondary control.

Modern solutions execute the tasks of secondary and tertiary control using a function LFC (Load and Frequency Controller) in control algorithms of SCADA–EMS (Energy Management System) that supports the system operator. Apart from controlling frequency and power interchanges, SCADA–EMS contains a number of other optimization and security management functions. A detailed description is beyond the scope of this book but interested readers are referred to Wood and Wollenberg (1996).

The hierarchical structure shown in Figure 9.12 also contains a block UTC corresponding to control of the synchronous time, that is time measured by synchronous clocks based on the system frequency. Power system frequency varies continuously, so synchronous clocks tend to have an error proportional to the integral of the system frequency. This error is eliminated by occasionally changing the reference value of the frequency.

In the European UCTE system the nominal frequency is $f_n = 50$ Hz . The synchronous time deviation is calculated at the control centre in Laufenberg (Switzerland) using the UTC time standard. On certain days of each month, the centre broadcasts a value of frequency correction to be inserted in secondary control systems in order to eliminate the synchronous time deviation. If synchronous clocks are delayed then the frequency correction is set to 0.01 Hz, that is the set frequency is $f_{ref} = 50.01$ Hz . If synchronous clocks are ahead then the frequency correction is set to -0.01 Hz, that is the set frequency is $f_{ref} = 49.99$ Hz. Usually the system operates for a few tens of days with a correction of -0.01 Hz, for a few days with $+0.01$ Hz and then without any correction for the remainder of the year.

Usually control areas are grouped in large interconnected systems with the central regulator of one area (usually the largest) regulating power interchanges in the given area with respect to other areas. In such a structure the central controller of each area regulates its own power interchanges while the central controller of the main area additionally regulates power interchanges of the whole group.

9.1.6 Defence Plan Against Frequency Instability

The system of frequency and power control discussed above is adequate for typical disturbances of a real power balance consisting of the unplanned outage of a large generating unit. The largest disturbance which can be handled by the system is referred to as the *reference incident*. In the European UCTE system, the reference incident consists of losing units with a total power of 3000 MW. Larger incidences have to handled by each system operator using its own defence plan together with appropriate facilities that defend the power system from the disturbance spreading out. Examples of such a defence plan are shown in Tables 9.1 and 9.2.

The defence plan described in these tables should be treated as an example. It is based on a paper by Kuczyński, Paprocki and Strzelbicki (2005) and also includes updates resulting from experience gained from the wide area disturbance in UCTE interconnected power systems on 4 November 2006. The interested reader is advised to check the UCTE Master Plan document at www.ucte.org.

Table 9.1 Example of a defence plan against a frequency drop

f (Hz)	Δf (Hz)	Type of defence action
50.000	<0.200	Normal operation with primary control with small dead zones (Figure 9.6a) and secondary control of frequency and tie-line power: $\text{ACE} = -\Delta P_{\text{tie}} - \lambda_{\text{R}} \Delta f$
49.800	0.200	Central secondary controllers of subsystems are blocked. Generating units operate only with primary control and manual setting of reference power
		Primary control hidden in units operating with large dead zones ± 200 mHz (Figure 9.6b) is automatically activated
		Switching of pumped storage plants from the pump mode to the generation mode
		Starting of fast-start units (diesel and open-cycle gas units)
49.000 48.700	1.000 1.300	Underfrequency load shedding (first two stages)
48.700	1.300	Turbine governors (primary control) switch from power regulation according to droop characteristic to speed control (Figure 9.6)
48.500 48.300 48.100	1.500 1.700 1.900	Underfrequency load shedding (next three stages)
47.500	2.500	Generating units are allowed to trip by turbine protection. The units supply their own ancillary services and demand of their islands (if they survived). System operators start system restoration by reconnecting the islands and lost generating units

Table 9.2 Example of a defence plan against frequency rise.

f(Hz)	Δf(Hz)	Type of defence action
51.500	1.500	Generating units are allowed to trip by turbine protection. The units supply their own ancillary services
51.300	1.300	Turbine governors (primary control) switch from power regulation according to droop characteristic to speed control (Figure 9.6)
50.200	0.200	Switching of pumped storage plants from the generation mode to the pump mode
		Stopping of fast-start units (diesel and open-cycle gas units)
		Primary control hidden in units operating with large dead zones ±200 mHz (Figure 9.6b) is automatically activated
		Central secondary controllers of subsystems are blocked. Generating units operate only with primary control and manual setting of reference power
50.000	<0.200	Normal operation with primary control with small dead zones (Figure 9.6a) and secondary control of frequency and the tie-line power: $\text{ACE} = -\Delta P_{\text{tie}} - \lambda_{\text{R}} \Delta f$

9.1.7 *Quality Assessment of Frequency Control*

The quality assessment of frequency and power interchange control can be divided into two types:

1. Quality assessment of the control during normal system operation.
2. Quality assessment during large disturbances such as unplanned outages of a generating unit.

Quality assessment during normal system operation is executed using the standard deviation of the frequency error:

$$\sigma = \sqrt{\frac{1}{n}\sum_{i=1}^{n}(f - f_{\text{ref}})^2}, \tag{9.13}$$

where n is the number of measurements. The measurements are taken every 15 min in a month. Additionally, a percentage share of frequency deviations higher than 50 mHz is calculated together with the times of their appearance.

Quality assessment of frequency control following a large disturbance is shown in Figure 9.13. The bold line shows an example of frequency changes following an unplanned outage of a large generating unit. There was a frequency error of Δf_0 just before the disturbance. The disturbance happened during a correction to the synchronous time when $f_{\text{ref}} = 50.01$ Hz . Following the disturbance, the frequency dropped by a maximum of Δf_2. Frequency control restored the frequency to the reference value within the allowed error. The whole range of frequency variations was limited to within an area shown by the dashed lines and referred to as the *trumpet characteristic*. The trumpet characteristic is made up of two exponential curves defined by

$$\begin{aligned} H(t) &= f_{\text{ref}} \pm A\,\mathrm{e}^{-t/T} \quad \text{for} \quad t \le 900 \text{ s} \\ H(t) &= \pm 20 \text{ mHz} \quad \text{for} \quad t \ge 900 \text{ s}, \end{aligned} \tag{9.14}$$

where the $\pm$ signs correspond to the upper and lower parts of the characteristic and A is the initial width. The exponential characteristic finishes when $t = 900$ s , that is $t = 15$ min . Then the

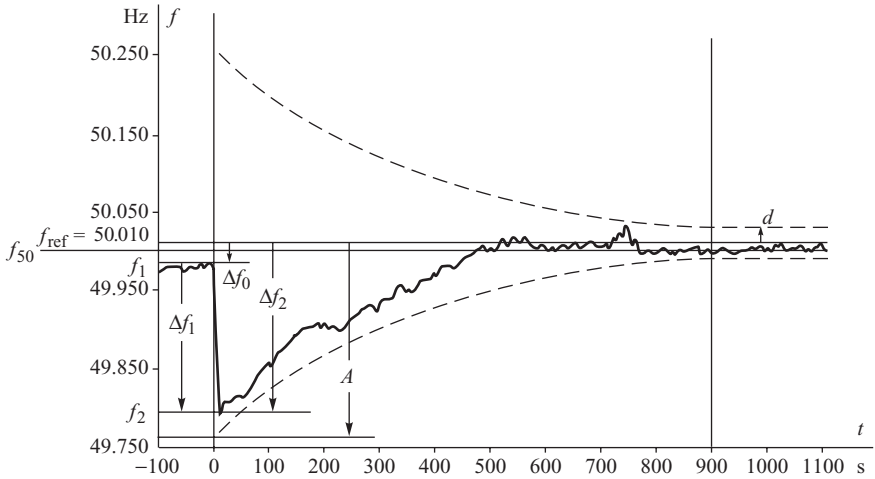

Figure 9.13 Illustration of the quality assessment of frequency control using a trumpet characteristic. Based on the document 'UCTE – Ground Rules – Supervision of the application of rules concerning primary and secondary control of frequency and active power in UCTE'. Reproduced by permission of UCTE.

characteristic consists of two horizontal lines limiting the frequency error to ±20 mHz corresponding to the required accuracy of frequency control during normal operation. The exponential curves must descend smoothly to the horizontal lines. For that to happen, the time constant of the exponential curves must be equal to

$$T = \frac{900}{\ln(A/d)}. \tag{9.15}$$

The initial width A depends on the disturbance size ΔP_0 according to

$$A = 1.2\left(\frac{|\Delta P_0|}{\lambda_R} + 0.030\right), \tag{9.16}$$

where λ_R is the frequency stiffness of the power system. As an example, if a unit of several hundred megawatts is tripped, the width of the trump characteristic, and therefore also the varying frequency error, is a few hundred millihertz.

If variations of frequency following a disturbance ΔP_0 are inside the trump characteristic then the frequency control is deemed to be satisfactory.

9.2 Stage I – Rotor Swings in the Generators

Having described the AGC, it is now possible to analyse the response of a power system to a power imbalance caused, for example, by the tripping of a generating unit. This response can be divided into four stages depending on the duration of the dynamics involved:

Stage I	Rotor swings in the generators (first few seconds)
Stage II	Frequency drop (a few seconds to several seconds)
Stage III	Primary control by the turbine governing systems (several seconds)
Stage IV	Secondary control by the central regulators (several seconds to a minute).

The dynamics associated with each of these four stages will be described separately in order to illustrate how they develop in the system. To begin the discussion the power system shown schematically in Figure 9.14a will be considered where a power station transmits its power to the system via two parallel transmission lines. The power station itself is assumed to consist of two identical generating units operating onto the same busbar. The disturbance considered will be the disconnection of one of the generating units. In Stage I of the disturbance the way in which the remaining generating unit contributes to the production of the lost power will be given special attention.

The sudden disconnection of one of the generators will initially produce large rotor swings in the remaining generating unit and much smaller rotor swings in the other generators within the system. For simplicity these small oscillations will be neglected to allow the rest of the system to be replaced by an infinite busbar. The time scale of the rotor swings is such that the generator transient model applies and the mechanical power supplied by the turbine remains constant. To simplify considerations, the classical model representation of the generator will be used, Equations (5.15) and (5.40). Figure 9.14b shows the equivalent predisturbance circuit diagram for the system. As both generators are identical they can be represented by the same transient emf $\underline{E}'$ behind an equivalent reactance that combines the generator transient reactance X'_d, the transformer reactance X_T and the system reactance X_s.

Figure 9.15 shows how the equal area criterion can be applied to this problem. In this diagram $P_-(\delta')$ and $P_+(\delta')$ are the transient power–angle characteristics, and P_{m-} and P_{m+} the mechanical powers, before and after the disturbance occurs. Initially the plant operates at point 1 and the equivalent power angle with respect to the infinite busbar is δ'_0. Disconnection of one of the generators has two effects. Firstly, the equivalent reactance of the system increases

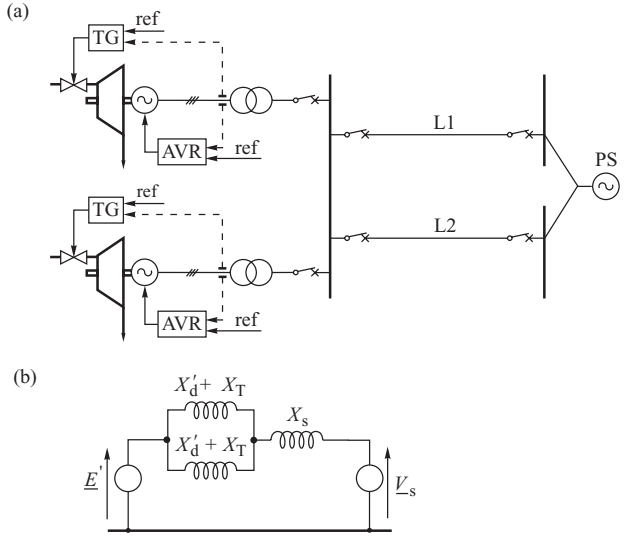

Figure 9.14 Parallel generating units operating onto an infinite busbar: (a) schematic diagram; (b) equivalent circuit.

so that the amplitude of the power–angle characteristic decreases. Consequently the pre- and postdisturbance power–angle characteristics are

$$P_-(\delta'_0) = \frac{E'V_s}{\frac{X'_d+X_T}{2} + X_s}\sin\delta'_0, \quad P_+(\delta'_0) = \frac{E'V_s}{X'_d + X_T + X_s}\sin\delta'_0. \tag{9.17}$$

Secondly, the mechanical power delivered to the system drops by an amount equal to the power of the lost unit, that is $P_{m+} = 0.5P_{m-}$.

As the rotor angle of the remaining generator cannot change immediately after the disturbance occurs, the electrical power of the generator is greater than the mechanical power delivered by

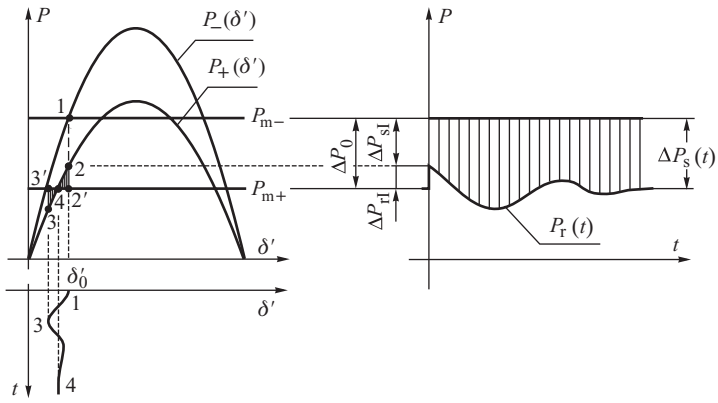

Figure 9.15 Application of the equal area criterion to determine the first stage of the dynamics. Duration of the phenomena – first few seconds.

its prime mover, point 2. The rotor is decelerated and loses kinetic energy corresponding to the area 2–2′–4. Due to its momentum the rotor continues to decrease its angle past point 4 until it stops at point 3 when the area 4–3–3′ equals the area 2–2′–4. The damping torques then damp out subsequent oscillations and the rotor tends towards its equilibrium point 4.

The amplitude of the rotor oscillations of any given generator will depend on the amount of lost generation it picks up immediately after the disturbance occurs. Using the notation of Figure 9.15 gives

$$\begin{aligned} \Delta P_0 &= P_-(\delta_0') - P_{m+} = P_{m-} - P_{m+} \\ \Delta P_{rI} &= P_+(\delta_0') - P_{m+} \\ \Delta P_{sI} &= \Delta P_0 - \Delta P_{rI}, \end{aligned} \tag{9.18}$$

where ΔP_0 is the lost generating power and ΔP_{rI} and ΔP_{sI} are the contributions of the generating units remaining in operation and of the system, respectively, in meeting the power imbalance ΔP_0 at the very beginning of the disturbance. The subscript 'I' indicates that these equations apply to Stage I of the disturbance. Using the first of the equations in (9.18), a formula for ΔP_{rI} can be rewritten as

$$\Delta P_{rI} = P_+(\delta_0') - P_{m+} = \left[P_+(\delta_0') - P_{m+}\right] \frac{1}{P_-(\delta_0') - P_{m+}} \Delta P_0. \tag{9.19}$$

Substituting (9.17) into (9.19) and noting that $P_{m+} = 0.5 P_{m-}$ gives

$$\Delta P_{rI} = \frac{1}{1+\beta} \Delta P_0, \tag{9.20}$$

where $\beta = (X_d' + X_T)/X_s$. The amount that the system contributes in order to meet the lost generation can now be calculated as

$$\Delta P_{sI} = \Delta P_0 - \Delta P_{rI} = \frac{\beta}{\beta+1} \Delta P_0, \tag{9.21}$$

with the ratio of the contributions (9.20) and (9.21) being

$$\frac{\Delta P_{rI}}{\Delta P_{sI}} = \frac{1}{\beta} = \frac{X_s}{X_d' + X_T}. \tag{9.22}$$

This equation shows that ΔP_r, the contribution of the unit remaining in operation in meeting the lost power, is proportional to the system equivalent reactance X_s. Both contributions ΔP_r and ΔP_s are depicted in Figure 9.15. Due to the fact that the inertia of the unit is much smaller than that of the power system, the generator quickly decelerates, loses kinetic energy, and both its rotor angle and generated power decrease (Figure 9.15b). As a consequence the power imbalance starts to increase and is met by the system which starts to increase its contribution ΔP_s. This power delivered by the system has been shaded in Figure 9.15 and, when added to the generator's share $P_r(t)$, must equal the load existing before the disturbance. As can be seen from this figure, the proportion of lost generation picked up by the system changes with time so that the system contributes more and more as time progresses.

Although the formula in Equation (9.22) has been derived for two parallel generating units operating in the system, a similar expression can be derived for the general multi-machine case. This expression would lead to a conclusion that is similar to the two-machine case in that at the beginning of Stage I of the dynamics the share of any given generator in meeting the lost load will depend on its electrical distance from the disturbance (coefficient β). In the case of Figure 9.14 the imbalance appeared at the power plant busbar. Thus X_s is a measure of the electrical distance of the system from the disturbance and $(X_d' + X_T)$ is a measure of the electrical distance of the unit remaining in operation.

9.3 Stage II – Frequency Drop

The situation shown in Figure 9.15 can only last for a few seconds before the power imbalance causes all the generators in the system to slow down and the system frequency to drop. Thus begins Stage II of the dynamics. During this stage the share of any one generator in meeting the power imbalance depends solely on its inertia and not on its electrical distance from the disturbance. Assuming that all the generators remain in synchronism, they will slow down at approximately the same rate after a few rotor swings in Stage I of the dynamics. This may be written as

$$\frac{\mathrm{d}\Delta\omega_1}{\mathrm{d}t} \approx \frac{\mathrm{d}\Delta\omega_2}{\mathrm{d}t} \approx \cdots \approx \frac{\mathrm{d}\Delta\omega_{N_\mathrm{G}}}{\mathrm{d}t} = \varepsilon, \tag{9.23}$$

where $\Delta\omega_i$ is the speed deviation of the ith generator, ε is the average acceleration and N_G is the number of generators.

According to the swing equation, Equation (5.14), the derivative of the speed deviation can be replaced by the ratio of the accelerating power ΔP_i of the ith unit over the inertia coefficient M_i. This modifies Equation (9.23) to

$$\frac{\Delta P_1}{M_1} \approx \frac{\Delta P_2}{M_2} \approx \cdots \approx \frac{\Delta P_n}{M_n} \approx \varepsilon. \tag{9.24}$$

If the change in the system load due to the frequency change is neglected, then the sum of the extra load taken by each generator must be equal to the power lost ΔP_0

$$\Delta P_0 = \sum_{i=1}^{N_\mathrm{G}} \Delta P_i. \tag{9.25}$$

Substituting the increment ΔP_i in this equation with $\Delta P_i = M_i\varepsilon$ gives

$$\Delta P_0 = \varepsilon \sum_{i=1}^{N_\mathrm{G}} M_i \quad \text{or} \quad \varepsilon = \frac{\Delta P_0}{\sum\limits_{i=1}^{N_\mathrm{G}} M_i} \quad \text{so that} \quad \Delta P_i = M_i\varepsilon = \frac{M_i}{\sum\limits_{k=1}^{N_\mathrm{G}} M_k}\Delta P_0. \tag{9.26}$$

This equation determines the contribution of the ith generator in meeting the lost power in Stage II of the dynamics when each generator contributes an amount of power proportional to its inertia. In practice the inertia constant H_i is similar for all the generators so that substituting for $M_i = 2H_iS_{\mathrm{n}i}/\omega_\mathrm{s}$ from Equation (5.13), then Equation (9.26) can be written as

$$\Delta P_i \approx \frac{S_{\mathrm{n}i}}{\sum\limits_{i=1}^{N_\mathrm{G}} S_{\mathrm{n}i}}\Delta P_0. \tag{9.27}$$

During Stage II the contribution of the generator remaining in operation and the rest of the power system in meeting the lost power can be expressed, using (9.26), as

$$\Delta P_{\mathrm{rII}} = \frac{M_\mathrm{r}}{M_\mathrm{r} + M_\mathrm{s}}\Delta P_0 \quad \text{and} \quad \Delta P_{\mathrm{sII}} = \frac{M_\mathrm{s}}{M_\mathrm{r} + M_\mathrm{s}}\Delta P_0. \tag{9.28}$$

Subscript II has been added here to emphasize that these equations are valid during Stage II. In a similar way as in Equation (9.22), the ratio of the contributions is

$$\frac{\Delta P_{\mathrm{rII}}}{\Delta P_{\mathrm{sII}}} = \frac{M_\mathrm{r}}{M_\mathrm{s}} \approx \frac{S_{\mathrm{nr}}}{S_{\mathrm{ns}}}, \tag{9.29}$$

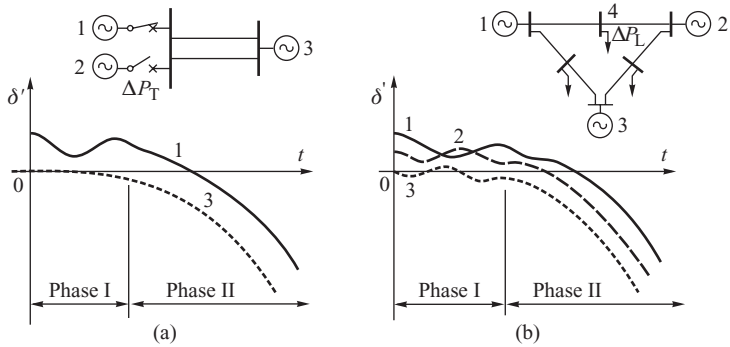

Figure 9.16 Examples of changes in the rotor angles in the case of a real power disturbance: (a) disconnection of generator 2; (b) sudden increase of the load at node 4. The duration of Stage II is a few to several seconds.

and is equal to the ratio of the inertia coefficients or, approximately, to the ratio of the rated powers. As $S_{ns} \gg S_{nr}$ (infinite busbar), the contribution by the generator remaining in operation in covering the lost power is very small. The assumption made when preparing Figure 9.15 was that $\Delta P_{rII} \approx \Delta P_0 S_{nr}/S_{ns} \approx 0$.

Figure 9.16a illustrates the case when the system has a finite equivalent inertia and the rotor angle of both the remaining generator and the system equivalent generator decreases as the frequency drops. The initial rotor angle oscillations are the same as those shown for the first stage of the dynamics in Figure 9.15. The angles then decrease together as the generators operate synchronously.

Figure 9.16b shows the case of a three-generator system where the load at node 4 suddenly increases. Generators 1 and 2 are close to the disturbance, so they participate more strongly in the first stage of the oscillations than does generator 3. During the second stage the power angles synchronously decrease and the system frequency drops.

9.4 Stage III – Primary Control

Stage III of the dynamics depends on how the generating units and the loads react to the drop in frequency. Section 2.2.3 explained how, as frequency (speed) drops, the turbine governor opens the main control valves to increase the flow of working fluid through the turbine and so increase the turbine mechanical power output. In the steady state, and during very slow changes of frequency, the increase in mechanical power for each generating unit is inversely proportional to the droop of the static turbine characteristic. Equations (9.4) and (9.6) can be rewritten as

$$\begin{aligned} P_T &= P_{T0} + \Delta P_T = P_{T0} - K_T \Delta f \frac{P_{T0}}{f_n} \\ P_L &= P_{L0} + \Delta P_L = P_{L0} + K_L \Delta f \frac{P_{L0}}{f_n}. \end{aligned} \tag{9.30}$$

The operating frequency of the system is determined by the point of intersection of these two characteristics.

Typical generation and load characteristics are shown in Figure 9.17 where the generation characteristic before the disturbance is denoted by P_{T-} and after by P_{T+}. If a generating unit is lost the system generation characteristic P_T moves to the left by the value of the lost power ΔP_0 and,

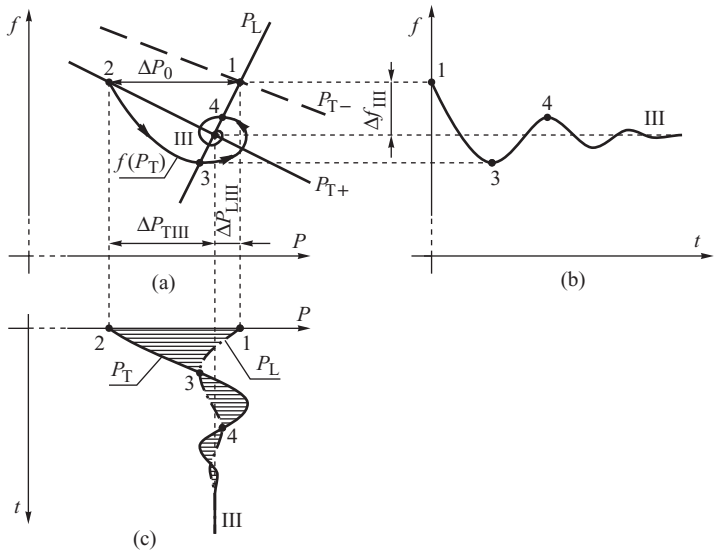

Figure 9.17 Stage III of the dynamics caused by an imbalance in real power: (a) the generation characteristic and the frequency response characteristic; (b) frequency changes; (c) power changes. The duration of Stage III is several seconds.

according to Equation (9.4), the slope of the characteristic increases slightly as a the value of K_T decreases.

Before the disturbance occurs, the system operates at point 1 corresponding to the intersection of the P_L and P_{T-} characteristics. After the generator is disconnected the frequency initially remains unchanged and the generation operating point is shifted to point 2. Then the generation tends to move towards point III which corresponds to the intersection of the P_L and P_{T+} characteristics but, because of the delay introduced by the time constants of the turbines and their governors, this point cannot be reached immediately. Initially the difference between the generated power, point 2, and the load power, point 1, is large and the frequency starts to drop as described in Stage I and Stage II of the dynamics. In Stage III the turbine reacts to the drop in frequency by increasing its power output but, because of the aforementioned time delays in the turbine regulator system, the trajectory of the turbine power $f(P_T)$ lies below the static generation characteristic P_{T+}. As the frequency drops, the generated power increases while the power taken by the load decreases. The difference between the load and the generation is zero at point 3. According to the swing equation, a zero value of deceleration power means

$$\frac{\mathrm{d}\Delta\omega}{\mathrm{d}t} = 2\pi \frac{\mathrm{d}\Delta f}{\mathrm{d}t} = 0, \tag{9.31}$$

and the frequency $f(t)$ reaches a local minimum, Figure 9.17b.

Because of the inherent inertia of the turbine regulation process, the mechanical power continues to increases after point 3 so that the generated power exceeds the load power and the frequency starts to rise. At point 4 the balance of power is again zero and corresponds to the local maximum in the frequency shown in Figure 9.17b. The oscillations continue until the steady-state value of the frequency f_{III} is reached at point III corresponding to the intersection of the P_L and P_{T+} static

characteristics. The value of f_{III} can be determined from Figure 9.17a

$$\Delta P_0 = \Delta P_{\mathrm{TIII}} - \Delta P_{\mathrm{LIII}} = -K_{\mathrm{T}} \frac{P_{\mathrm{L}}}{f_{\mathrm{n}}} \Delta f_{\mathrm{III}} - K_{\mathrm{L}} \frac{P_{\mathrm{L}}}{f_{\mathrm{n}}} \Delta f_{\mathrm{III}} = -P_{\mathrm{L}} \left(K_{\mathrm{T}} + K_{\mathrm{L}}\right) \frac{\Delta f_{\mathrm{III}}}{f_{\mathrm{n}}}, \tag{9.32}$$

with the frequency error f_{III} being

$$\frac{\Delta f_{\mathrm{III}}}{f_{\mathrm{n}}} = \frac{-1}{K_{\mathrm{T}} + K_{\mathrm{L}}} \frac{\Delta P_0}{P_{\mathrm{L}}} \quad \text{or} \quad \frac{\Delta f_{\mathrm{III}}}{f_{\mathrm{n}}} = \frac{-1}{K_{\mathrm{f}}} \frac{\Delta P_0}{P_{\mathrm{L}}}, \tag{9.33}$$

where the coefficient $K_{\mathrm{f}} = K_{\mathrm{T}} + K_{\mathrm{L}}$ is the system stiffness introduced in Equation (9.7). Figure 9.17c shows how the generated power and the load power change during this period. The difference between the two is shaded and corresponds to the power that decelerates ($P_{\mathrm{T}} < P_{\mathrm{L}}$) or accelerates ($P_{\mathrm{T}} > P_{\mathrm{L}}$) the rotor.

For the system shown in Figure 9.14 the contributions of the generator remaining in operation and that of the system in covering the lost generation in Stage III of the dynamics can be obtained from Equation (9.4) as

$$\Delta P_{\mathrm{rIII}} = -K_{\mathrm{Tr}} \frac{\Delta f_{\mathrm{III}}}{f_{\mathrm{n}}} P_{\mathrm{nr}}, \quad \Delta P_{\mathrm{sIII}} = -K_{\mathrm{Ts}} \frac{\Delta f_{\mathrm{III}}}{f_{\mathrm{n}}} P_{\mathrm{ns}}, \tag{9.34}$$

where the subscript III is added to emphasize that these equations are valid during Stage III of the dynamics. The ratio of contributions resulting from these equations is

$$\frac{\Delta P_{\mathrm{rIII}}}{\Delta P_{\mathrm{sIII}}} = \frac{K_{\mathrm{Tr}}}{K_{\mathrm{Ts}}} \frac{P_{\mathrm{nr}}}{P_{\mathrm{ns}}} \approx \frac{P_{\mathrm{nr}}}{P_{\mathrm{ns}}}. \tag{9.35}$$

The approximate equality in this equation is valid when the droop of all the turbine characteristics is approximately the same. In practice the ratios (9.35) and (9.29) are very similar. This physically corresponds to the fact that, during the transition period between the second and third stages, the generator is in synchronism with the system and there are no mutual oscillations between them.

9.4.1 The Importance of the Spinning Reserve

The discussion so far has assumed that, within the range of frequency variations, each of the generating units has a linear turbine characteristic and that the overall generation characteristic is also linear. In practice each generating unit must operate within the limits that are placed on its thermal and mechanical performance. To ensure that these limits are adhered to, its governing system is equipped with the necessary facilities to make certain that the unit does not exceed its maximum power limit or the limit placed on the speed at which it can take up power. These limits can have a substantial impact on how a unit behaves when the system frequency changes.

Figure 9.3 showed how the spinning reserve, and its allocation in the system, influences the shape of the generation characteristic. In order to help quantify the influence of spinning reserve, the following coefficients are defined:

$$r = \frac{\sum_{i=1}^{N_{\mathrm{G}}} P_{\mathrm{n}i} - P_{\mathrm{L}}}{P_{\mathrm{L}}}, \quad p = \frac{\sum_{i=1}^{R} P_{\mathrm{n}i}}{\sum_{i=1}^{N_{\mathrm{G}}} P_{\mathrm{n}i}}, \tag{9.36}$$

where $\sum_{i=1}^{N_{\mathrm{G}}} P_{\mathrm{n}i}$ is the sum of the power ratings of all the generating units connected to the system and $\sum_{i=1}^{R} P_{\mathrm{n}i}$ is the sum of the power ratings of all the units operating on the linear part of their characteristics; that is, loaded below their power limit. The coefficient r is the *spinning reserve*

coefficient and defines the relative difference between the maximum power capacity of the system and the actual load.

A simple expression for the local droop of the generation characteristic can be obtained by assuming that the droop of all the units which are not fully loaded are approximately identical, that is $\rho_i = \rho$ and $K_i = K = 1/\rho$. For the units operating at their limits, $\rho_i = \infty$ and $K_i = 0$. Under these conditions

$$\begin{aligned}\Delta P_{\mathrm{T}} &= -\sum_{i=1}^{N_{\mathrm{G}}} K_i P_{\mathrm{n}i} \frac{\Delta f}{f_{\mathrm{n}}} = -\sum_{i=1}^{R} K_i P_{\mathrm{n}i} \frac{\Delta f}{f_{\mathrm{n}}} \cong -K \sum_{i=1}^{R} P_{\mathrm{n}i} \frac{\Delta f}{f_{\mathrm{n}}} \\ &= -Kp \sum_{i=1}^{N_{\mathrm{G}}} P_{\mathrm{n}i} \frac{\Delta f}{f_{\mathrm{n}}} = -Kp\,(r+1)\,P_{\mathrm{L}} \frac{\Delta f}{f_{\mathrm{n}}}.\end{aligned} \tag{9.37}$$

Dividing by P_{L} gives

$$\frac{\Delta P_{\mathrm{T}}}{P_{\mathrm{L}}} = -K_{\mathrm{T}} \frac{\Delta f}{f_{\mathrm{n}}}, \tag{9.38}$$

where

$$K_{\mathrm{T}} = p\,(r+1)\,K \quad \text{and} \quad \rho_{\mathrm{T}} = \frac{\rho}{p\,(r+1)}. \tag{9.39}$$

Equation (9.38) is similar to Equation (9.4) and describes the linear approximation of the nonlinear generation characteristic for a given load. The local droop ρ_{T} increases as the spinning reserve decreases. At the limit, when the load P_{L} is equal to the system generating capacity, both the coefficients r and p are zero and $\rho_{\mathrm{T}} = \infty$. This corresponds to all the generating units being fully loaded.

The influence of the spinning reserve on the frequency drop in Stage III of the dynamics can now be determined. For the linear approximation to the generator characteristic given in Equation (9.38) the drop in frequency can be determined from Equation (9.33) as

$$\frac{\Delta f_{\mathrm{III}}}{f_{\mathrm{n}}} = \frac{-1}{p\,(r+1)\,K + K_{\mathrm{L}}} \frac{\Delta P_0}{P_{\mathrm{L}}}, \tag{9.40}$$

indicating that the smaller the spinning reserve coefficient r, the bigger the drop in frequency due to the loss of power ΔP_0. With a large spinning reserve the static characteristic $P_{\mathrm{T}(1)}$ shown in Figure 9.18 has a shallow slope and the drop in frequency is small. On the other hand, when the spinning reserve is small, the $P_{\mathrm{T}(2)}$ characteristic is steep, and the frequency drop is increased for the same power disturbance ΔP_0. In the extreme case when no spinning reserve is available, the

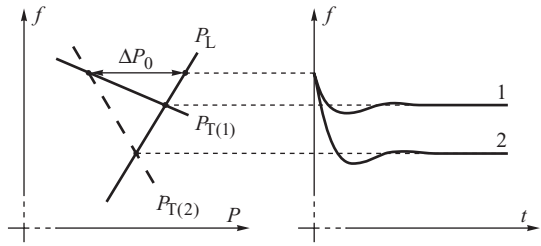

Figure 9.18 The influence of spinning reserve on the frequency drop due to a power imbalance: 1, large spinning reserve; 2, small spinning reserve.

generating units would be unable to increase their generation and the whole power imbalance ΔP_0 could only be covered by the frequency effect of the loads. As the frequency sensitivity K_L of the loads is generally small, the frequency drop would be very high.

Equation (9.37) defines the way in which each of the generating units contributes to the power imbalance at the end of Stage III with Equation (9.38) quantifying the net effect of the primary turbine control in meeting the lost load.

Example 9.1

Consider a 50 Hz system with a total load $P_L = 10\,000$ MW in which $p = 60\,\%$ of the units give $r = 15\,\%$ of the spinning reserve. The remaining 40 % of the units are fully loaded. The average droop of the units with spinning reserve is $\rho = 7\,\%$ and the frequency sensitivity coefficient of the loads is $K_L = 1$. If the system suddenly loses a large generating unit of $\Delta P_0 = 500$ MW, calculate the frequency drop and the amount of power contributed by the primary control.

From Equation (9.39) $K_T = 0.6(1 + 0.15)1/0.07 = 9.687$ and, according to Equation (9.33), primary control will give the frequency drop in Stage III as

$$\Delta f_{III} = \frac{-1}{9.867 + 1} \times \left[\frac{500}{10\,000}\right] \times 50 \approx 0.23 \text{ Hz},$$

where the turbine governor primary control contributes

$$\Delta P_{T\,III} = 9.867 \times \frac{0.23}{50} \times 10\,000 = 454 \text{ MW},$$

with the remaining deficit of

$$\Delta P_{L\,III} = 1 \times \frac{0.23}{50} \times 10\,000 = 46 \text{ MW},$$

being covered by the frequency effect of the loads. If there were no spinning reserve, the deficit would be covered entirely by the frequency effect of the loads giving a frequency drop of

$$\Delta f_{III} = \frac{-1}{0 + 1} \times \left[\frac{500}{10\,000}\right] \times 50 = 2.5 \text{ Hz},$$

which is about 10 times greater than in the case with (only) 15 % spinning reserve.

9.4.2 Frequency Collapse

Spinning reserve is much more important than is suggested by the approximate formula in Equation (9.40). In practice the power output of the turbine is frequency dependent so that if the frequency is much lower than the nominal frequency the turbine power will be less than that given by Equation (9.38) and the frequency may drop further and further until the system suffers a *frequency collapse*.

The hidden assumption made in the generation characteristics of Figure 9.18 is that when a unit is fully loaded the mechanical driving power delivered by the turbine does not depend on the frequency deviation. This assumption is only true for small frequency deviations while a larger frequency drop reduces mechanical power due to a deterioration in the performance of boiler feed pumps, see Section 2.2.3. In this case the static generation characteristic takes the form shown in Figure 9.13. Adding the power–frequency characteristics of individual generating units now gives the system generation characteristic P_T shown in Figure 9.19.

On the upper part of the generation characteristic the local droop at each point is positive and depends on the system load according to the formulae given in (9.39). The lower part of the characteristic corresponds to the decrease in the power output due to the deterioration in the

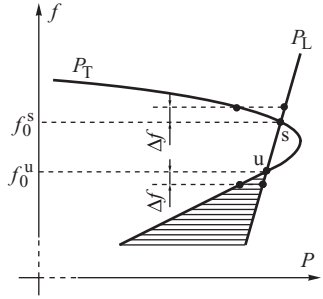

Figure 9.19 The static generation and load characteristics of the power system and the equilibrium points: s, locally stable equilibrium point; u, locally unstable equilibrium point.

performance of the boiler feed pumps. For a given load frequency characteristic P_L the inflexion in the generation characteristic produces two equilibrium points. At the upper point s any small disturbance that produces an increase in the frequency $\Delta f > 0$ will result in the load power exceeding the generation power; the generators are decelerated and the system returns to the equilibrium point s. Similarly, any small disturbance that causes a decrease in frequency will result in the generation power exceeding the load power, the rotors accelerate, the frequency increases and the system again returns to the equilibrium point. Point s is therefore *locally stable* because for any small disturbance within the vicinity of this point the system returns to point s. The region in which this condition holds is referred to as the *area of attraction*.

In contrast the lower point u is *locally unstable* because any disturbance within the vicinity of this point will result in the system moving away from the equilibrium point. The region in which this happens is referred to as the *area of repulsion*. For example, if a disturbance reduces the frequency $\Delta f < 0$ then the system moves into the shaded area below point u, the generated power is reduced so that the system load is greater than the system generation, the rotors decelerate and the frequency drops further.

With these qualifications of turbine performance in mind, assume that the system operates with a low spinning reserve at point 1 on Figure 9.20. A loss ΔP_0 in generation now occurs and the operating point moves from point 1 to point 2. The excess load over generation is large and produces an initial rapid drop in frequency. As the difference between the load and generation reduces, the rate at which the frequency drops slows down and the system generation trajectory $f(P_T)$ approaches the equilibrium point u. When the trajectory $f(P_T)$ enters the area of repulsion of point u it is forced away and the system suffers a frequency collapse.

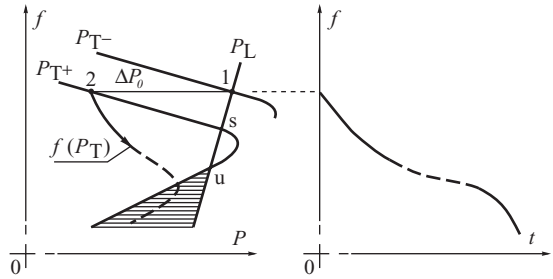

Figure 9.20 An example of frequency collapse.

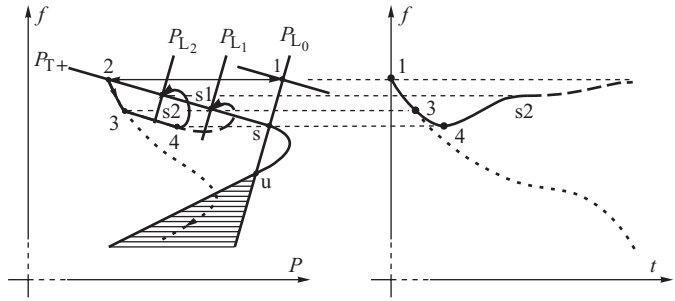

Figure 9.21 Two-stage load shedding to protect against frequency collapse.

The frequency collapse illustrated in Figure 9.20 occurred following the *sudden* appearance of the power imbalance ΔP_0. Had the system generation characteristic changed slowly from P_{T+} to P_{T-} by gradually reducing the generation, then it would have met the locally stable points and stayed there. Obviously if the power imbalance ΔP_0 is greater than the spinning reserve then the postdisturbance demand characteristic P_L lies to the right of the nose of the generation characteristic P_{T+} and the frequency would collapse regardless of how sudden the power change was.

9.4.3 Underfrequency Load Shedding

Many systems can be protected from frequency collapse by importing large blocks of power from neighbouring systems to make up for the lost generation. However, in an islanded system, or in an interconnected system with a shortage of tie-line capacity, this will not be possible and the only way to prevent a frequency collapse following a large disturbance is to employ *automatic load shedding*.

Automatic load shedding is implemented using underfrequency relays. These relays detect the onset of decay in the system frequency and shed appropriate amounts of system load until the generation and load are once again in balance and the power system can return to its normal operating frequency. Load shedding relays are normally installed in distribution and subtransmission substations as it is from here that the feeder loads can be controlled.

As load shedding is a somewhat drastic control measure, it is usually implemented in stages with each stage triggered at a different frequency level to allow the least important loads to be shed first. Figure 9.21 shows the effect of load shedding when a power imbalance ΔP_0 appears on a system with a low spinning reserve. Without load shedding the system would suffer a frequency collapse as shown by the dotted line. The first stage of load shedding is activated at point 3 and limits the load to a value corresponding to characteristic P_{L_1}. The rate of frequency drop is now much slower as the difference between the load and generation is smaller. At point 4 the second stage of load shedding is triggered, further reducing the load to a value corresponding to characteristic P_{L_2}. Generation is now higher than the load, the frequency increases, and the system trajectory tends towards point s2 where the P_{L_2} and P_{T+} characteristics intersect.

Besides protecting against frequency collapse, load shedding may also be used to prevent deep drops in system frequency.

9.5 Stage IV – Secondary Control

In Stage IV of the dynamics, the drop in system frequency and the deviation in the tie-line power flows activate the central AGC, the basic operation of which has been described in Section 9.1.

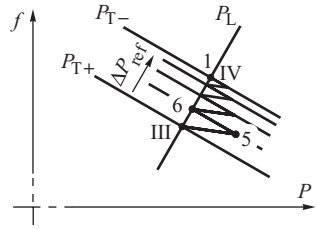

Figure 9.22 Stepped shifting of the generation characteristic by a slow-acting central regulator.

9.5.1 Islanded Systems

In an islanded system there are no tie-line connections to neighbouring systems so that the central regulator controls only the system frequency. As the frequency drops, the central regulator transmits control signals to the participating generating units to force them to increase their power output. This lifts the system generation characteristic in the (f, P) plane.

Figure 9.22 illustrates the action of a very slow-acting central regulator which transmits its first control signal at the end of Stage III corresponding to point III. This first control signal shifts the generation characteristic upwards a small amount so that at a given frequency, point 5, there is an excess of generation over load. The generators start to accelerate and the frequency increases until point 6 is reached. The central regulator now sends a further signal to increase power output and the generation characteristic is shifted further up. After a few such steps point IV is reached at which the frequency returns to its reference value and the central regulator ceases operating.

Although the zigzag line in Figure 9.22 is only a rough approximation to the actual trajectory, it illustrates the interaction between the secondary control action of the central regulator, which shifts the generation characteristic upwards, and the primary control action of the turbine governing systems, which moves the operating point along the static generation characteristic. In a real power system the inertia within the power regulation process ensures smooth changes in the power around the zigzag line to produce the type of response shown in Figure 9.23. Stages I, II and III of the frequency change are as described in the previous sections and, at the end of Stage III, the trajectory tends to wrap itself around the temporary equilibrium point III, Figure 9.23a, but does not settle at this point. The AGC of Stage IV now comes into operation and the trajectory tends towards the new equilibrium point IV. Although the difference between the frequency at points III and IV is small, the central regulator acts slowly so that correction of the frequency drop during Stage IV of the dynamics may take a long time as shown by the broken curves in Figure 9.23b and c.

If the central frequency control acts faster than as shown in Figure 9.23, it will come into operation before the end of Stage III. The trajectory $f(P_T)$ does not now wrap around point III and the frequency starts to increase earlier as shown by curve 2 in Figure 9.24.

The way in which the frequency is returned to its nominal value depends on the dynamics of the central regulator shown in Figure 9.10 and defined by Equation (9.12). The regulator dynamics consist of proportional and integral action, both of which increase the regulator output signal ΔP_{ref} as the frequency drops. The amount of integral action is determined by the integral time constant T_R while the proportional action is dependent on the coefficient β_R. Careful selection of these two coefficients ensures that the frequency returns smoothly to its reference value as shown in Figure 9.24. Particularly problematic is a small integral time constant, because the smaller is this time constant, the faster the regulation signal increases. This can be compensated to some extent by the coefficient β_R which will start to decrease the signal ΔP_{ref} as soon as the frequency starts to rise. In the extreme case of small values of β_R and T_R the response is underdamped and the reference frequency value will be reached in an oscillatory way.

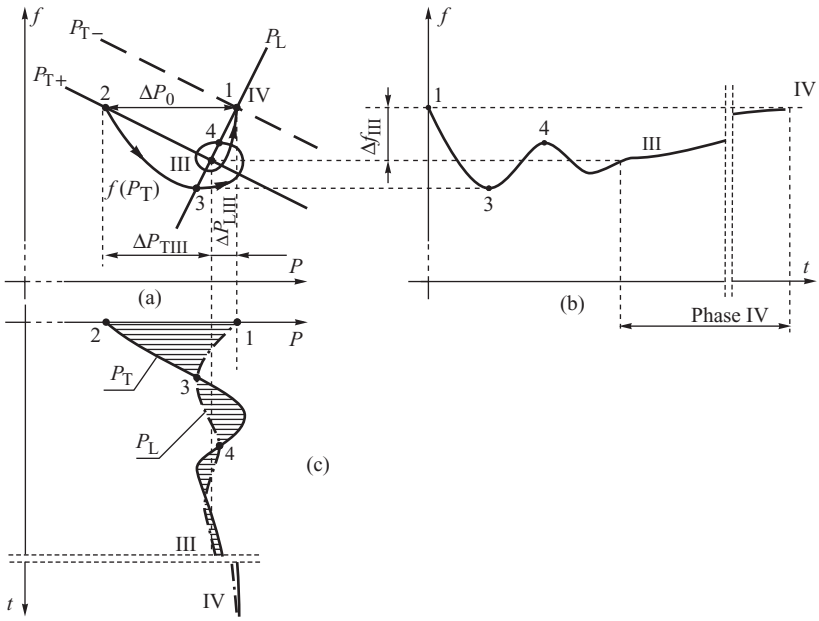

Figure 9.23 Stages III and IV of the frequency variations produced by a disturbance in the balance of real power: (a) generation and load characteristics and the system trajectory; (b) changes in frequency; (c) changes in power. The time duration of Stage IV is several seconds to a minute.

Section 9.1 explained how not all the generating units necessarily participate in AGC. This means that only a part of the spinning reserve can be activated by the central regulator during secondary control. That part of the spinning reserve that belongs to the generators participating in secondary control is referred to as the *available regulation power*.

If the available regulation power is less than the lost power, then Stage IV of the dynamics will terminate when all the available regulation power has been used. This corresponds to the system trajectory settling at an equilibrium point somewhere between points III and IV on Figure 9.23 at a frequency that is lower than the reference value. The system operators may now verbally instruct other generating stations not on central control to increase their power output to help remove the frequency offset. In the case of a large power deficit, further action would consist of connecting new generating units from the cold reserve which, when connected, will release the capacity controlled by the central regulator. The frequency changes associated with this process are very slow and are not considered here.

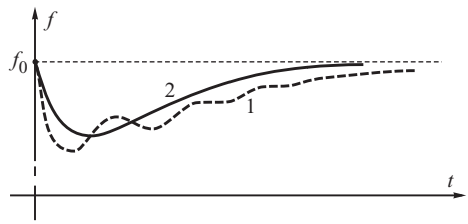

Figure 9.24 Examples of changes in frequency: 1, with a slow central regulator; 2, with a fast central regulator.

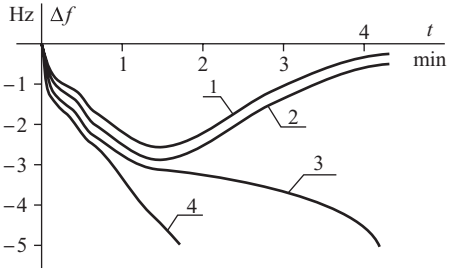

Figure 9.25 An example of the frequency variations when $\Delta P_0 = 10\,\%\Delta P_L$. Curve 1 corresponds to $r = 16\,\%$; 2 corresponds to $r = 14\,\%$; 3 corresponds to $r = 12\,\%$; and 4 corresponds to $r = 8\,\%$.

Equation (9.35) defines the contribution of each of the generating units in covering the power imbalance at the end of Stage III. In Stage IV the increase in generation is enforced by the central regulator and the contribution of each unit, and the ratio $\Delta P_{rIV}/\Delta P_{sIV}$, will depend on whether or not the particular generating unit participates in central control.

Provided that the spinning reserve and the available regulation power are large enough, then in many cases they can prevent the system suffering a frequency collapse. Figure 9.25 shows an example of how the frequency variations depend on the value of the spinning reserve coefficient. The disturbance consists of losing generation ΔP_0 equivalent to 10 % of the total load power P_L. In the first two cases $r \geq 14\,\%$ and the frequency returns to its reference value thanks to the operation of primary and secondary control. The third case corresponds to the frequency collapse shown in Figure 9.20. In the fourth case there is no intersection point between the generation and the load characteristic and the frequency quickly collapses.

9.5.1.1 The Energy Balance over the Four Stages

When a power system loses a generating unit it loses a source of both electrical and mechanical energy. By the end of the power system dynamic response, this lost energy has been recovered as illustrated in Figure 9.26. The upper bold curve shows the variations of the mechanical power provided by the system while the lower bold curve shows the variations of electrical power of the loads due to frequency variations. All these variations are similar to those shown in Figure 9.23c. Initially the energy shortfall is produced by converting the kinetic energy of the rotating masses of the generating units and the loads to electrical energy, area 1 and area 2. This reduction in kinetic

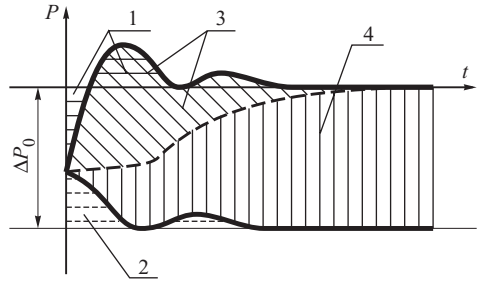

Figure 9.26 Share of the individual components in covering the power imbalance: 1, rotating masses of the generating units; 2, rotating masses of the loads; 3, primary control; 4, secondary control. Based on Welfonder (1980). Reproduced by permission of E. Welfoner.

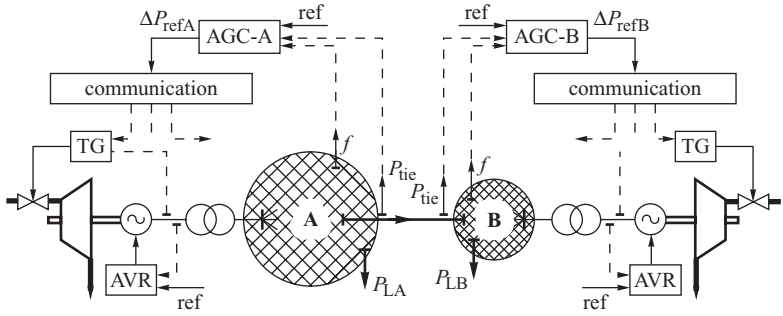

Figure 9.27 The functional diagram of an interconnected system consisting of two subsystems: a big system A and a small system B.

energy causes a drop in frequency which activates the turbine governor primary control so that the mechanical energy supplied to the system is increased but at a lower frequency, area 3. This energy is used partially to generate the required energy shortfall, and partially to return the kinetic energy borrowed from the rotating masses. Secondary control then further increases the mechanical energy, area 4, which is used to generate the required additional electrical energy and to increase the kinetic energy of the rotating masses so restoring the system frequency.

9.5.2 Interconnected Systems and Tie-Line Oscillations

This discussion will be limited to the interconnected system shown in Figure 9.27 consisting of two subsystems of disproportionate size, system A and system B, referred to as the big system and the small system respectively. The tie-line interchange power P_{tie} will be assumed to flow from the big system to the small system and an imbalance of power ΔP_0 assumed to arise in the small system. During the first three stages of the dynamics the influence of the central regulators in both system A and system B may be neglected.

Both systems are replaced by an equivalent generator, as in Figure 9.14b, to obtain the equivalent circuit of Figure 9.28a. In this circuit the reactance X combines the reactances of the tie-line connecting the two systems, the equivalent network reactance of both systems and the transient reactances of all the generators. As one of the subsystems is large compared with the other, the generator–infinite busbar model and the equal area criterion can be used to analyse Stage I of the dynamics.

The power–angle characteristic $P_{\text{B}}(\delta')$ of the small system is a sinusoid, corresponding to a power transfer between the systems, shifted by a constant value corresponding to the power demand in the small system P_{LB}. It is assumed that system B imports power from A so that $P_{\text{TB}} < P_{\text{LB}}$ and its power angle is negative with respect to system A. Before the disturbance occurs, the system operates at point 1 corresponding to the intersection of the $P_{\text{B}}(\delta')$ characteristic and the horizontal line representing the mechanical power $P_{\text{TB}-}$. The small system now loses generation equal to ΔP_0 and the power generated in this system drops to $P_{\text{TB}+}$. The electrical power exceeds the mechanical power and the rotors of the generators in system B slow down. The equivalent system rotor moves from point 1 to point 2 and then to point 3 in Figure 9.28b. Along this motion the electrical power generated in system B decreases and, as a result, additional power starts to flow from system A, Figure 9.28d. The maximum change in the value of the instantaneous power in the tie-lines increases to almost double the value of the lost power, the difference between points 1 and 3. Oscillations in the power begin during which kinetic energy in both systems is used to cover the lost generation. The angular velocities of the generator rotors drop and the system enters Stage II of the dynamics.

Stage I of the dynamics is dangerous from a stability point of view in that if the area 1–1′–2 is greater than the area 2–3–4 then the system loses stability and the small system will operate

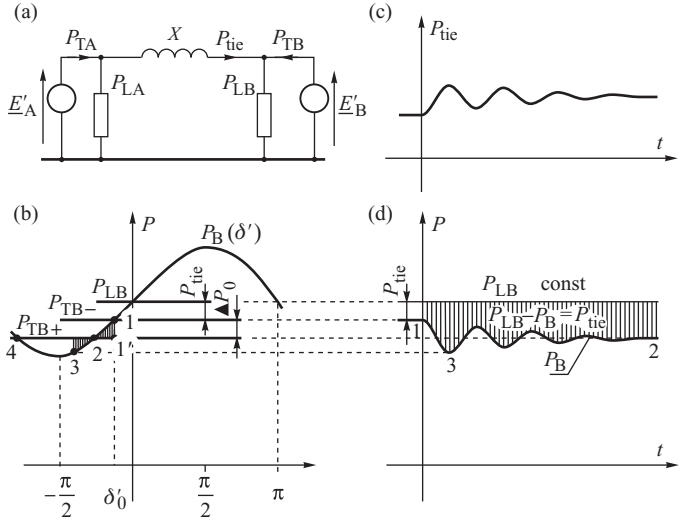

Figure 9.28 Application of the equal area criterion to determine the tie-line power during the first stage of the dynamics: (a) equivalent circuit; (b) the power–angle characteristic taking into account equivalent loads; (c) changes in the tie-line power; (d) changes in the generated power. The time duration of the phenomena is a few seconds.

asynchronously with respect to the big system with $\omega_B < \omega_A$. Such a situation may occur when the tie-line capacity is small and the disturbance in power balance large. During asynchronous operation large oscillations in the power tie-line power will occur with the difference between the maximum and the minimum value being twice the amplitude of the sinusoid shown in Figure 9.28b. As the possibility of resynchronizing the systems is small, they would usually be disconnected to avoid damaging equipment in either system.

In Stage II the power imbalance is covered in proportion to the inertia coefficients of the equivalent systems as determined by Equations (9.28), that is

$$\Delta P_{AII} = \frac{M_A}{M_A + M_B}\Delta P_0 \quad \text{and} \quad \Delta P_{BII} = \frac{M_B}{M_A + M_B}\Delta P_0, \tag{9.41}$$

where $M_A = \sum_{i=1}^{N_{GA}} M_i$ and $M_B = \sum_{i=1}^{N_{GB}} M_i$ are the sums of the inertia coefficients of the rotating masses in each system. Equations (9.41) suggest that the big system A will almost entirely cover the power imbalance since $M_A \gg M_B$, so in Stage II of the frequency variations $\Delta P_{tieII} \approx \Delta P_0$ and the tie-lines will be additionally loaded with a value of the power lost in system B.

At the end of Stage III the frequency drops by a value Δf_{III} that can be calculated from the system stiffness K_f defined in Equation (9.33). ΔP_0 is given by

$$\Delta P_0 = (\Delta P_{TAIII} - \Delta P_{LAIII}) + (\Delta P_{TBIII} - \Delta P_{LBIII}), \tag{9.42}$$

and, when substituting the values for K_{TA}, K_{LA}, K_{TB} and K_{LB} obtained from Equations (9.39) and (9.6), a similar formula to that in Equation (9.33) for the frequency drop in Stage III is obtained:

$$\frac{\Delta f_{III}}{f_n} = \frac{-1}{K_{fA}P_{LA} + K_{fB}P_{LB}}\Delta P_0, \tag{9.43}$$

where $K_{fA} = K_{TA} + K_{LA}$ and $K_{fB} = K_{TB} + K_{LB}$ are the stiffnesses of the big and the small system respectively. The increase in the tie-line interchange can be determined from a power balance on

one of the systems, in this case the big system A, when

$$\begin{aligned}\Delta P_{\text{tieIII}} &= \Delta P_{\text{TAIII}} - \Delta P_{\text{LAIII}} = -\left(K_{\text{TA}} + K_{\text{LA}}\right) P_{\text{LA}} \frac{\Delta f_{\text{III}}}{f_{\text{n}}} \\ &= -K_{\text{fA}} P_{\text{LA}} \frac{\Delta f_{\text{III}}}{f_{\text{n}}} = \frac{K_{\text{fA}} P_{\text{LA}}}{K_{\text{fA}} P_{\text{LA}} + K_{\text{fB}} P_{\text{LB}}} \Delta P_0.\end{aligned} \tag{9.44}$$

Under the assumption that $P_{\text{LA}} \gg P_{\text{LB}}$ this formula simplifies to $\Delta P_{\text{tieIII}} \approx \Delta P_0$ when, during Stage III, the tie-line power interchange is increased by the value of the lost power, as during Stage II. Such an increase in the power flow may result in system instability when the interconnected systems split into two asynchronously operating subsystems. Also, with such a large power transfer the thermal limit on the line may be exceeded when the overcurrent relays trip the line, again leading to asynchronous operation of both systems.

Assuming that the tie-line remains intact, the increase in the tie-line interchange power, combined with the drop of frequency, will force the central regulators in both systems to intervene. The ACE at the end of Stage III can be calculated from Equation (9.11) using the formulae given in Equations (9.43) and (9.44) as

$$\text{ACE}_{\text{A}} = -\Delta P_{\text{tieIII}} - \lambda_{\text{RA}} \Delta f_{\text{III}} \quad \text{and} \quad \text{ACE}_{\text{B}} = +\Delta P_{\text{tieIII}} - \lambda_{\text{RB}} \Delta f_{\text{III}}. \tag{9.45}$$

As explained in Section 9.1 (Equation (9.10)), the ideal regulator bias settings are

$$\lambda_{\text{RA}} = K_{\text{fA}} \frac{P_{\text{LA}}}{f_{\text{n}}} \quad \text{and} \quad \lambda_{\text{RB}} = K_{\text{fB}} \frac{P_{\text{LB}}}{f_{\text{n}}}, \tag{9.46}$$

but this is difficult to achieve in practice as the values of the stiffnesses K_{fA} and K_{fB} can only be estimated. Consequently, assuming that K_{RA} and K_{RB} are estimates of K_{fA} and K_{fB} respectively, then the bias settings are

$$\lambda_{\text{RA}} = K_{\text{RA}} \frac{P_{\text{LA}}}{f_{\text{n}}} \quad \text{and} \quad \lambda_{\text{RB}} = K_{\text{RB}} \frac{P_{\text{LB}}}{f_{\text{n}}}, \tag{9.47}$$

and Equations (9.45) become

$$\text{ACE}_{\text{A}} = -\Delta P_{\text{tieIII}} - \lambda_{\text{RA}} \Delta f_{\text{III}} = \frac{-K_{\text{fA}} P_{\text{LA}} + K_{\text{RA}} P_{\text{LA}}}{K_{\text{fA}} P_{\text{LA}} + K_{\text{fB}} P_{\text{LB}}} \Delta P_0, \tag{9.48}$$

$$\text{ACE}_{\text{B}} = +\Delta P_{\text{tieIII}} - \lambda_{\text{RB}} \Delta f_{\text{III}} = \frac{K_{\text{fA}} P_{\text{LA}} + K_{\text{RB}} P_{\text{LB}}}{K_{\text{fA}} P_{\text{LA}} + K_{\text{fB}} P_{\text{LB}}} \Delta P_0. \tag{9.49}$$

9.5.2.1 Ideal Settings of the Regulators

Assume that the stiffnesses K_{fA} and K_{fB} of both systems are known and that the central regulator bias settings λ_{RA} and λ_{RB} are selected such that

$$K_{\text{RA}} = K_{\text{fA}}, \quad K_{\text{RB}} = K_{\text{fB}}. \tag{9.50}$$

In this case, Equations (9.48) and (9.49) give

$$\text{ACE}_{\text{A}} = 0 \quad \text{and} \quad \text{ACE}_{\text{B}} = \Delta P_0, \tag{9.51}$$

and the central regulator of the big system, system A, will not demand an increase in the power generation in its area. Only the small system will increase its generation in order to cover its own power imbalance. If the available regulation power in the small system is high enough to cover the lost generation then the big system will not intervene at all and, as the generation in the small system is increased, the tie-line power interchange will drop to its scheduled value.

The value of the system stiffness $K_f = K_T + K_L$ is never constant because it depends on the composition of the system load and generation and on the spinning reserve. Consequently, the condition defined by Equation (9.50) is almost never satisfied and the central regulator of the bigger system will take part in the secondary control to an amount defined by Equation (9.48).

Example 9.2

An interconnected system consists of two subsystems of different size. The data of the subsystems are: f_n= 50 Hz, P_{LA}=37 500 MW, $K_{TA} = 8$ (ρ_{TA}= 0.125), $K_{LA} \approx 0$, $K_{RA} = K_{TA}$, $P_{LB} = 4000$ MW, $K_{TB} = 10$ ($\rho_{TB} = 0.1$), $K_{LB} \approx 0$, $K_{RB} = K_{TB}$.

Two large generating units are suddenly lost in the smaller system producing a power deficit of $\Delta P_0 = 1300$ MW, that is 32.5 % of the total generation in this subsystem. The resulting frequency and power variations for both subsystems, assuming no limits on the power generation (linear generation characteristics), are shown in Figure 9.29.

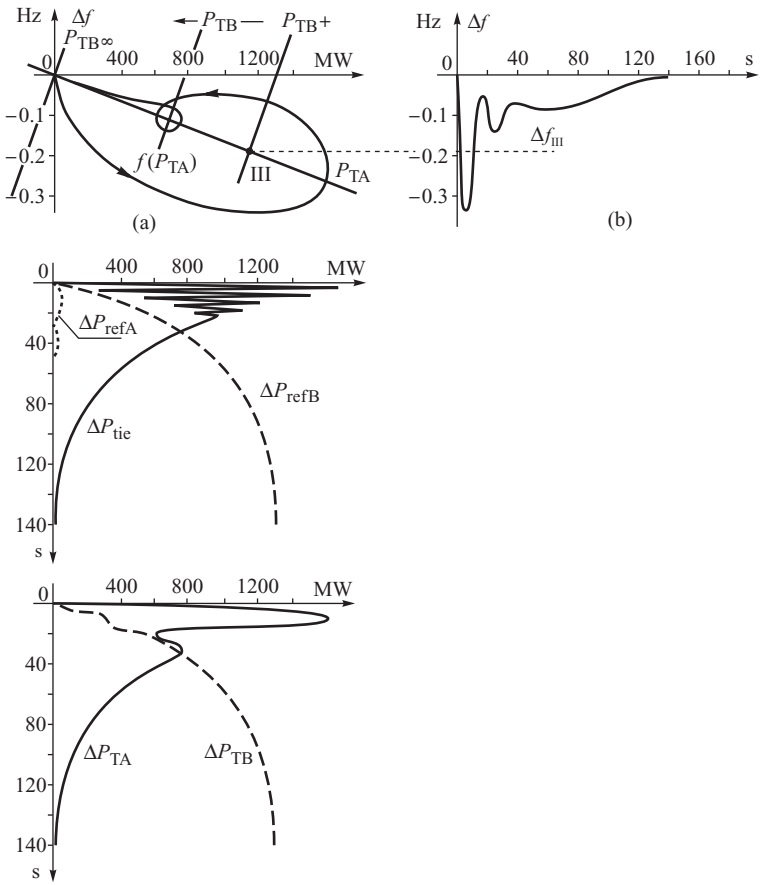

Figure 9.29 Illustration for Example 9.2: (a) the static characteristics of both systems and the trajectory $f(P_{TA})$; (b) frequency variations; (c) tie-line power interchange oscillations and the change of power demanded by the central regulators of both subsystems; (d) change in the mechanical power supplied by the turbines.

The characteristic P_{TA} has a small slope corresponding to $K_{TA}P_{LA}/f_n = 6000$ MW/Hz. The slope of the characteristic of the smaller system is much higher and corresponds to $K_{TB}P_{LB}/f_n = 800$ MW/Hz. The characteristic P_{TB+} is inverted and shifted by $\Delta P_0 = 1300$ MW, so that intersection of the characteristics P_{TB+} and P_{TA} determines the frequency deviation Δf_{III} at point III. The central regulator of the small system acts fast enough for the P_{TB} characteristic to move so that point III is not reached. Further action due to the integral term in the regulator shifts the characteristic P_{TB} slowly to the position $P_{TB\infty}$ corresponding to nominal frequency.

It is worth noting the small frequency oscillations characteristic of the third stage of the dynamics. Because of the fast-acting central regulator, these oscillations take place above the value Δf_{III}, Figure 9.29b. The tie-line power flow initially increases very quickly in Stage I of the dynamics, and then oscillates around the scheduled value increased by the value of the lost generation. The period of oscillations is around 3 s. Then, as the central regulator in the small system enforces an increase in the generation, the tie-line flow slowly decreases to its scheduled value.

The central PI regulator quite quickly creates the output signal ΔP_{refB} as shown in Figure 9.29c. The generating units respond to this increased power demand by increasing the generation by ΔP_{TB}, Figure 9.29d. Because of the primary turbine control, the mechanical power of the big system P_{TA} initially increases to cover the power imbalance and then quickly drops to the instantaneous equilibrium point corresponding to the end of Stage III. After that P_{TA} slowly decreases as the generation P_{TB}, forced by secondary control, increases. At the same time the frequency increases so that the frequency error of the central regulator of the big system becomes negligibly small and the regulator becomes inactive.

9.5.2.2 Non-Ideal Settings of the Central Regulator

If $K_{RA} > K_{fA}$, then the signal $\lambda_{RA}\Delta f$ is initially larger than the signal ΔP_{tie} and the regulator tries to increase the generation in system A. Although the increased generation speeds up the rate at which the frequency increases, it slows down the rate at which the tie-line error ΔP_{tie} decreases and in some cases can lead to a temporary increase in this error. Consequently, the signal ΔP_{tie} becomes greater than the signal $\lambda_{RA}\Delta f$ and the central regulator starts to reduce the generation in system A, so essentially withdrawing this subsystem from secondary control.

If $K_{RA} < K_{fA}$, then the signal ΔP_{tie} is initially higher than the signal $\lambda_{RA}\Delta f$ and the regulator of the big system tries to reduce its generation despite the fact that the frequency is smaller than nominal. This drop in generation is not desirable from the frequency regulation point of view but does reduce the tie-line flows. When $\lambda_{RA}\Delta f$ becomes larger than ΔP_{tie} the regulator will start to increase the recently reduced generation so as to re-establish the required power in system A.

In both the above cases the inaccuracy of the frequency bias setting causes unnecessary intervention of the bigger system in covering the generation loss in the smaller system. In the above example a large amount of regulation power was available so that use of the non-ideal regulator settings was not dangerous. However, should the amount of regulation power available be insufficient to cover the lost power then the consequence of non-ideal regulator settings becomes more significant as described below.

9.5.2.3 Insufficient Available Regulation Power

When the available regulation power ΔP_{regB} in the small system is less than the generation loss ΔP_0 then system B is unable to cover the power loss on its own and the big system A must intervene to cover part of the lost power. Initially the dynamics are identical to the case in which the regulation power in the small system was unlimited. The difference between the two cases appears when the small system has used up all its available regulation power. Further changes can only take place via regulation of the big system. Its central regulator is now subject to two error signals of opposite

sign (Figure 9.12). The signal $\lambda_{RA}\Delta f$ generated by the frequency error demands an increase in the generation while the signal ΔP_{tie} generated by the tie-line power deviation demands a decrease in the generation. The regulation process terminates when the signals balance each other and the total error signal is zero. Denoting the final steady-state values of the error signals as Δf_∞ and $\Delta P_{tie\infty}$, the regulation equation is

$$\mathrm{ACE_A} = -\Delta P_{tie\,\infty} - K_{RA} P_{LA} \frac{\Delta f_\infty}{f_n} = 0. \tag{9.52}$$

On the other hand, the tie-line power interchange must satisfy the overall power balance of the small system

$$\Delta P_0 - \Delta P_{regB} = \Delta P_{tie\,\infty} - (K_{TB} + K_{LB})\, P_{LB} \frac{\Delta f_\infty}{f_n}. \tag{9.53}$$

Physically this means that the power imbalance in the small system B may be covered partly by an increase in the power imported from the big system A, partly by a change in internal generation and partly by a decreased demand resulting from the frequency drop in the whole interconnected system. Solving Equations (9.52) and (9.53) gives

$$\Delta P_{tie\infty} = \frac{K_{RA} P_{LA}}{K_{RA} P_{LA} + K_{fB} P_{LB}} \left(\Delta P_0 - \Delta P_{regB}\right), \tag{9.54}$$

$$\frac{\Delta f_\infty}{f_n} = -\frac{1}{K_{RA} P_{LA} + K_{fB} P_{LB}} \left(\Delta P_0 - \Delta P_{regB}\right). \tag{9.55}$$

Under the assumption that $P_{LA} \gg P_{LB}$ Equations (9.54) and (9.55) may be simplified to

$$\Delta P_{tie\,\infty} \cong \left(\Delta P_0 - \Delta P_{regB}\right), \tag{9.56}$$

$$\frac{\Delta f_\infty}{f_n} \cong -\frac{1}{K_{RA} P_{LA}} (\Delta P_0 - \Delta P_{regB}). \tag{9.57}$$

Additional validity is given to this simplification if the small system is fully loaded ($\Delta P_{regB} = 0$ and $K_{TB} = 0$) when the stiffness $K_{fB} = K_{TB} + K_{LB}$ has a small value corresponding to the frequency sensitivity of the loads K_{LB}. In this situation the whole power imbalance is covered by the tie-line interchange.

The frequency deviation Δf_∞ is inversely proportional to the coefficient $\lambda_{RA} = K_{RA} P_{LA}/f_n$ set at the central regulator. If the available regulation power is not large enough then too low a setting of the central regulator produces a steady-state frequency error. If $K_{RA} = K_{fA}$ then the final value of the frequency will correspond to the frequency level at which the available regulation power of the small system has run out. If $K_{RA} > K_{fA}$ then the regulator of the big system will increase its generation, decreasing the frequency error and allowing the tie-line interchange error to increase. If $K_{RA} < K_{fA}$, then the regulator of the big system will decrease its generation, increasing the frequency error, and the tie-line interchange error will not be allowed to increase. This can be illustrated by the following example.

Example 9.3

The available regulating power of the small subsystem considered in Example 9.2 is $\Delta P_{regB} = 500$ MW. The settings of the central regulators are $K_{RA} = 5.55 < K_{TA}$ and $K_{RB} = 12.5 > K_{TB}$. Neglecting the frequency sensitivity of the load, Equations (9.56) and (9.57) give: $\Delta P_{tie\infty} =$ 800 MW and $\Delta f_\infty = -0.16$ Hz. The power and frequency variations are illustrated in Figure 9.30. During the first 20 s of the disturbance the trajectory is the same as the one shown in

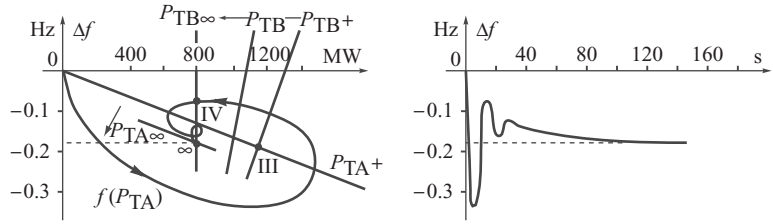

Figure 9.30 Illustration for Example 9.3.

Figure 9.29, but now the characteristic P_{TB} eventually settles at $P_{TB\infty}$. Trajectory $f(P_{TA})$ begins to wrap around the instantaneous equilibrium point IV, but the big system regulator decreases its generation shifting the characteristic from position P_{TA+} to position $P_{TA\infty}$. The dynamics end up at point ∞ where the frequency of the interconnected system is lower, by about $\Delta f_\infty = -0.16$ Hz, than the required value. A small portion of the trajectory $f(P_{TA})$, between point IV and ∞, corresponds to a slow reduction of frequency over several tens of seconds. The variations in the tie-line power interchange are similar to those shown in Figure 9.29, but settle down at a level corresponding to point ∞, that is $\Delta P_{tie\infty} = 800$ MW (the generation lost was $\Delta P_0 = 1300$ MW).

If the tie-line power interchange determined by Equation (9.54) is greater than the maximal thermal capacity of the tie-line, then the line will be tripped and the systems separated. The imbalance of power in the small system will cause a further drop in frequency which, in the absence of automatic load shedding, may lead to frequency collapse in that subsystem.

9.6 FACTS Devices in Tie-Lines

Series FACTS devices, described in Section 2.4.4, may be installed in tie-lines linking control areas in an interconnected power system. Their main function is execution of steady-state control functions described in Section 3.6. During the transient state caused by a sudden disturbance of a power balance in one of the subsystems, series FACTS devices installed in the tie-lines may affect the values of tie-line power interchanges P_{tie} and therefore also the value of the ACE given by (9.11) and the dynamics of secondary control executed by the central regulator shown in Figure 9.10. Hence a proper control algorithm and proper parameter selection have to be implemented at the regulator of the series FACTS device so that the control does not deteriorate the frequency and tie-line power interchange regulation process. This problem will be discussed in detail using as an example a thyristor-controlled phase angle regulator (TCPAR) which, from the power system point of view, acts as a fast phase shifting transformer.

A schematic diagram of a TCPAR regulator is shown in Figure 9.31. An integral-type regulator with negative feedback is placed in the main control path. The task of the regulator is to regulate real power flow in the line in which the FACTS device is installed. The reference value is supplied from the supervisory control system. A supplementary control loop devoted to damping of power swings and improving power stability is shown in the lower part of the diagram.

From the point of view of power system dynamics, an important problem for a series FACTS device installed in a tie-line is the control algorithm executing the supplementary control loop ensuring damping of interarea power swings in such a way that the frequency control executed by the central LFC regulator is not disturbed. The control algorithm described in this section is based on Nogal (2008).

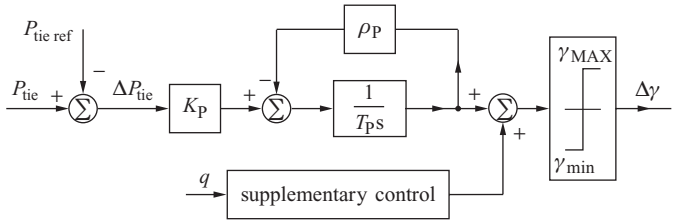

Figure 9.31 Power flow controller installed in a tie-line of an interconnected power system.

9.6.1 Incremental Model of a Multi-Machine System

Figure 9.32 illustrates the stages of developing a model of a phase shifting transformer installed in a tie-line. A booster voltage, which is in quadrature to the supply voltage, is injected in the transmission line using a booster transformer:

$$\Delta V_{\text{P}} = \gamma V_{\text{a}}, \tag{9.58}$$

where γ is the controlled variable. The booster transformer reactance has been added to the equivalent line reactance. To simplify considerations, the line and transformer resistances have been neglected.

The following relationships can be derived using the phasor diagram of Figure 9.32:

$$\sin\theta = \frac{\Delta V_{\text{P}}}{V_{\text{c}}} = \frac{\gamma V_{\text{a}}}{V_{\text{c}}}; \quad \cos\theta = \frac{V_{\text{a}}}{V_{\text{c}}}; \quad \delta_{\text{cb}} = \delta_{\text{ab}} + \theta. \tag{9.59}$$

According to Equation (3.15), real power flowing through a transmission line is given by

$$P_{\text{ab}} = P_{\text{cb}} = \frac{V_{\text{c}} V_{\text{b}}}{X} \sin\delta_{\text{cb}}. \tag{9.60}$$

Substituting (9.59) gives

$$\begin{aligned} P_{\text{ab}} &= \frac{V_{\text{c}} V_{\text{b}}}{X} \sin(\delta_{\text{ab}} + \theta) = \frac{V_{\text{c}} V_{\text{b}}}{X} (\sin\delta_{\text{ab}} \cos\theta + \cos\delta_{\text{ab}} \sin\theta) \\ &= \frac{V_{\text{a}} V_{\text{b}}}{X} \sin\delta_{\text{ab}} + \gamma \frac{V_{\text{a}} V_{\text{b}}}{X} \cos\delta_{\text{ab}}. \end{aligned} \tag{9.61}$$

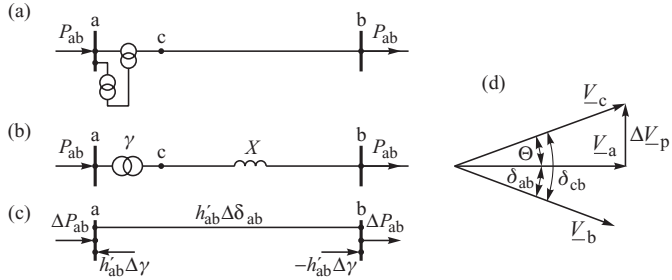

Figure 9.32 Stages of developing an incremental model of a transmission line with a phase shifting transformer: (a) one-line diagram; (b) admittance model with ideal transformation ratio; (c) incremental model; (d) phasor diagram.

This equation can also be written as

$$P_{ab} = b_{ab} \sin \delta_{ab} - b_{ab} \cos \delta_{ab} \gamma(t), \tag{9.62}$$

where $b_{ab} = V_a V_b / X$ is the amplitude of the power–angle characteristic of the transmission line.

The values of variables at a given operating point are $(\hat{P}_{ab}, \hat{\delta}, \hat{\gamma})$. Using these values, Equation (9.62) gives

$$\hat{P}_{ab} = b_{ab} \sin \hat{\delta}_{ab} - b_{ab} \cos \hat{\delta}_{ab} \hat{\gamma}. \tag{9.63}$$

The tie-line flow in (9.62) depends on both the power angle δ_{ab} and the quadrature transformation ratio $\gamma(t)$. Taking that into account and differentiating (9.62) in the vicinity of the operating point gives

$$\Delta P_{ab} = \left. \frac{\partial P_{ab}}{\partial \delta_{ab}} \right|_{\delta_{ab} = \hat{\delta}_{ab}} \Delta \delta_{ab} + \left. \frac{\partial P_{ab}}{\partial \gamma} \right|_{\gamma = \hat{\gamma}} \Delta \gamma. \tag{9.64}$$

Hence, taking into account (9.62),

$$\Delta P_{ab} = \left(b_{ab} \cos \hat{\delta}_{ab} + \hat{\gamma} \, b_{ab} \sin \hat{\delta}_{ab} \right) \Delta \delta - \left(b_{ab} \cos \hat{\delta}_{ab} \right) \Delta \gamma. \tag{9.65}$$

The coefficients $b_{ab} \cos \hat{\delta}_{ab}$ and $b_{ab} \sin \hat{\delta}_{ab}$ in this equation are the same as those in (9.63). Component $b_{ab} \sin \hat{\delta}_{ab}$ can be eliminated from (9.65) using (9.63) in the following way. Equation (9.63) gives

$$b_{ab} \sin \hat{\delta}_{ab} = \hat{P}_{ab} + \hat{\gamma} b_{ab} \cos \hat{\delta}_{ab}, \tag{9.66}$$

or

$$\hat{\gamma} b_{ab} \sin \hat{\delta}_{ab} = \hat{\gamma} \hat{P}_{ab} + \hat{\gamma}^2 b_{ab} \cos \hat{\delta}_{ab}. \tag{9.67}$$

Substituting this equation into (9.65) gives

$$\Delta P_{ab} = \left[\left(1 + \hat{\gamma}^2\right) \left(b_{ab} \cos \hat{\delta}_{ab} \right) + \hat{\gamma} \hat{P}_w \right] \Delta \delta_{ab} - \left(b_{ab} \cos \hat{\delta}_{ab} \right) \Delta \gamma. \tag{9.68}$$

The following notation is now introduced:

$$h_{ab} = \left. \frac{\partial P_{ab}}{\partial \delta_{ab}} \right|_{\delta_{ab} = \hat{\delta}_{ab}, \, \hat{\gamma} = 0} = b_{ab} \cos \hat{\delta}_{ab}, \tag{9.69}$$

$$h'_{ab} = \left(1 + \hat{\gamma}^2\right) \left(b_{ab} \cos \hat{\delta}_{ab} \right) + \hat{\gamma} \hat{P}_{ab} = \left(1 + \hat{\gamma}^2\right) h_{ab} + \hat{\gamma} \hat{P}_{ab}. \tag{9.70}$$

The variable h_{ab} given by (9.69) corresponds to the mutual synchronizing power for the line ab calculated neglecting the booster transformer. On the other hand, h'_{ab} given by (9.70) corresponds to the synchronizing power when the booster transformer has been taken into account. Using that notation, Equation (9.68) takes the form

$$\Delta P_{ab} = h'_{ab} \, \Delta \delta_{ab} - h_{ab} \, \Delta \gamma. \tag{9.71}$$

Equation (9.71) describes the incremental model of the transmission line shown in Figure 9.32c. There is an equivalent transmission line between nodes ‘a’ and ‘b’. A change in the flow in that line corresponds to a change in the voltage angles at both nodes. Nodal power injections correspond to flow changes due to regulation of the quadrature transformation ratio $\gamma(t)$. The power injections

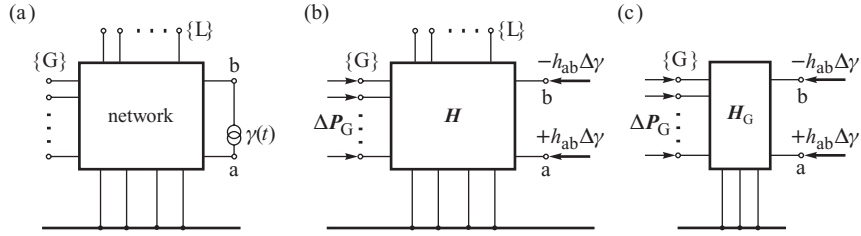

Figure 9.33 Stages of developing the incremental model: (a) admittance model with a phase shifting transformer; (b) incremental model; (c) incremental model after elimination of nodes {L}.

in nodes 'a' and 'b' are $+h_{ab}\,\Delta\gamma$ and $-h_{ab}\,\Delta\gamma$, respectively. To understand this, note that (9.71) holds for node 'a' while the same equation for node 'b' is

$$h'_{ab}\,\Delta\delta_{ab} = \Delta P_{ab} + h_{ab}\,\Delta\gamma. \tag{9.72}$$

It will be shown later that the derived incremental model of a branch with a phase shifting transformer is convenient for network analysis, especially for large networks, because it models changes in the quadrature transformation ratio by changes in power injections without changing the parameters of the branches.

Equation (3.157) derived in Section 3.6 modelled the effect of small changes of nodal voltages in a network. In analysing system frequency regulation, one can assume that changes in voltage magnitudes can be neglected and only changes in voltage angles are considered. Then Equation (3.157) takes the form

$$\Delta\boldsymbol{P} \cong \boldsymbol{H}\Delta\boldsymbol{\delta}, \tag{9.73}$$

where $\Delta\boldsymbol{P}$ and $\Delta\boldsymbol{\delta}$ are the vectors of changes in real power injections and voltage angles, respectively. Matrix $\boldsymbol{H}$ is the Jacobi matrix and consists of the partial derivatives $H_{ij} = \partial P_i/\partial\delta_j$. Equation (9.73) describes the *incremental model* of a network. Including a phase shifting transformer in incremental model of a network is illustrated in Figure 9.33. There are the following node types:

- {G} – generator nodes behind transient generator reactances;
- (L} – load nodes;
- a,b – terminal nodes of a line with a phase shifting transformer (as in Figure 9.32).

The line with the phase shifting transformer, Figure 9.33, is modelled using a transformation ratio and a branch. In the incremental model shown in Figure 9.33 this line is modelled in the same way as shown in Figure 9.32. Matrix $\boldsymbol{H}$ describing that network includes branch h'_{ab} from the incremental line model with the phase shifting transformer. There are real power injections in nodes 'a' and 'b', similar to Figure 9.32c, corresponding to flow changes due to transformation ratio regulation $\gamma(t)$.

Now Equation (9.73) describing the model shown in Figure 9.33b can be expanded as

$$\begin{matrix}\{\mathrm{G}\}\\ \mathrm{a}\\ \mathrm{b}\\ \{\mathrm{L}\}\end{matrix}\begin{bmatrix}\Delta\boldsymbol{P}_{\mathrm{G}}\\ \hline +h_{ab}\Delta\gamma\\ \hline -h_{ab}\Delta\gamma\\ \hline \mathbf{0}\end{bmatrix} \cong \begin{bmatrix}\\ \boldsymbol{H}\\ \\ \end{bmatrix}\begin{bmatrix}\Delta\boldsymbol{\delta}_{\mathrm{G}}\\ \hline \Delta\delta_{\mathrm{a}}\\ \hline \Delta\delta_{\mathrm{b}}\\ \hline \Delta\boldsymbol{\delta}_{\mathrm{L}}\end{bmatrix}. \tag{9.74}$$

Substitution $\Delta \boldsymbol{P}_{\mathrm{L}} = 0$ has been made on the left hand side of (9.74) because loads at $\{\mathrm{L}\}$ nodes are modelled as constant powers. Eliminating variables related to load nodes $\{\mathrm{L}\}$ in (9.74) by using the partial inversion method shown in Appendix A.2 makes it possible to transform Equation (9.74) to the following form:

$$\begin{matrix}\{\mathrm{G}\}\\ \mathrm{a}\\ \mathrm{b}\end{matrix}\left[\begin{array}{c}\Delta \boldsymbol{P}_{\mathrm{G}}\\ \hline +h_{\mathrm{ab}}\Delta\gamma\\ \hline -h_{\mathrm{ab}}\Delta\gamma\end{array}\right] \cong \left[\begin{array}{c|c|c}\boldsymbol{H}_{\mathrm{GG}} & \boldsymbol{H}_{\mathrm{Ga}} & \boldsymbol{H}_{\mathrm{Gb}}\\ \hline \boldsymbol{H}_{\mathrm{aG}} & H_{\mathrm{aa}} & H_{\mathrm{ab}}\\ \hline \boldsymbol{H}_{\mathrm{bG}} & H_{\mathrm{ba}} & H_{\mathrm{bb}}\end{array}\right]\left[\begin{array}{c}\Delta\boldsymbol{\delta}_{\mathrm{G}}\\ \hline \Delta\delta_{\mathrm{a}}\\ \hline \Delta\delta_{\mathrm{b}}\end{array}\right]. \tag{9.75}$$

This equation can be further transformed by partial inversion to the following equations:

$$\Delta \boldsymbol{P}_{\mathrm{G}} \cong \boldsymbol{H}_{\mathrm{G}}\Delta\boldsymbol{\delta}_{\mathrm{G}} + \left[\begin{array}{c|c}\boldsymbol{K}_{\mathrm{Ga}} & \boldsymbol{K}_{\mathrm{Gb}}\end{array}\right]\left[\begin{array}{c}+h_{\mathrm{ab}}\ \Delta\gamma\\ \hline -h_{\mathrm{ab}}\ \Delta\gamma\end{array}\right], \tag{9.76}$$

$$\left[\begin{array}{c}\Delta\delta_{\mathrm{a}}\\ \hline \Delta\delta_{\mathrm{b}}\end{array}\right] \cong -\left[\begin{array}{c}\boldsymbol{K}_{\mathrm{aG}}\\ \hline \boldsymbol{K}_{\mathrm{bG}}\end{array}\right]\Delta\boldsymbol{\delta}_{\mathrm{G}} + \left[\begin{array}{c|c}H_{\mathrm{aa}} & H_{\mathrm{ab}}\\ \hline H_{\mathrm{ba}} & H_{\mathrm{ba}}\end{array}\right]^{-1}\left[\begin{array}{c}+h_{\mathrm{ab}}\ \Delta\gamma\\ \hline -h_{\mathrm{ab}}\ \Delta\gamma\end{array}\right], \tag{9.77}$$

where

$$\boldsymbol{H}_{\mathrm{G}} = \boldsymbol{H}_{\mathrm{GG}} - \left[\begin{array}{c|c}\boldsymbol{H}_{\mathrm{Ga}} & \boldsymbol{H}_{\mathrm{Gb}}\end{array}\right]\left[\begin{array}{c|c}H_{\mathrm{aa}} & H_{\mathrm{ab}}\\ \hline H_{\mathrm{ba}} & H_{\mathrm{ba}}\end{array}\right]^{-1}\left[\begin{array}{c}\boldsymbol{H}_{\mathrm{aG}}\\ \hline \boldsymbol{H}_{\mathrm{bG}}\end{array}\right], \tag{9.78}$$

$$\left[\begin{array}{c|c}\boldsymbol{K}_{\mathrm{Ga}} & \boldsymbol{K}_{\mathrm{Gb}}\end{array}\right] = \left[\begin{array}{c|c}\boldsymbol{H}_{\mathrm{Ga}} & \boldsymbol{H}_{\mathrm{Gb}}\end{array}\right]\left[\begin{array}{c|c}H_{\mathrm{aa}} & H_{\mathrm{ab}}\\ \hline H_{\mathrm{ba}} & H_{\mathrm{ba}}\end{array}\right]^{-1} \tag{9.79}$$

$$\left[\begin{array}{c}\boldsymbol{K}_{\mathrm{aG}}\\ \hline \boldsymbol{K}_{\mathrm{bG}}\end{array}\right] = \left[\begin{array}{c|c}H_{\mathrm{aa}} & H_{\mathrm{ab}}\\ \hline H_{\mathrm{ba}} & H_{\mathrm{ba}}\end{array}\right]^{-1}\left[\begin{array}{c}\boldsymbol{H}_{\mathrm{aG}}\\ \hline \boldsymbol{H}_{\mathrm{bG}}\end{array}\right]. \tag{9.80}$$

Equations (9.76) and (9.77) describe the incremental model shown in Figure 9.33c. The former describes how a change in the transformation ratio of a phase shifting transformer affects power changes in all power system generators. The latter describes the influence of changes in the transformation ratio on the voltage angle changes in the terminal nodes of the line with the phase shifting transformer.

Equation (9.76) can be transformed to

$$\Delta \boldsymbol{P}_{\mathrm{G}} \cong \boldsymbol{H}_{\mathrm{G}}\ \Delta\boldsymbol{\delta}_{\mathrm{G}} + \Delta\boldsymbol{K}_{\mathrm{ab}}\ h_{\mathrm{ab}}\ \Delta\gamma, \tag{9.81}$$

where

$$\Delta\boldsymbol{K}_{\mathrm{ab}} = \boldsymbol{K}_{\mathrm{Ga}} - \boldsymbol{K}_{\mathrm{Gb}}. \tag{9.82}$$

Hence a power change in the ith generator can be expressed as

$$\Delta P_i \cong \sum_{j\in\{\mathrm{G}\}} H_{ij}\ \Delta\delta_j + \Delta K_i\ h_{\mathrm{ab}}\ \Delta\gamma, \tag{9.83}$$

where $\Delta K_i = K_{i\mathrm{a}} - K_{i\mathrm{b}}$. Thus, if $K_{i\mathrm{a}} \cong K_{i\mathrm{b}}$ then changes in $\Delta\gamma$ cannot influence power changes in the ith generator. In other words, that generator cannot be controlled using that phase shifting transformer. Coefficients $K_{i\mathrm{a}}$, $K_{i\mathrm{b}}$ can be treated as measures of the distance from nodes 'a' and 'b' to the ith generator. This means that if nodes 'a' and 'b' are at the same distance from the ith generator then the device cannot influence the generator. This can be checked using Figure 9.33c,

since power injections in nodes 'a' and 'b' have opposite signs. Hence if the distances are the same, then the influences on that generator cancel each other out.

The swing equation describing increments of rotor angles, Equation (5.15) in Section 5.1, is

$$\begin{aligned} \frac{\mathrm{d}\Delta\delta_i}{\mathrm{d}t} &= \Delta\omega_i \\ M_i \frac{\mathrm{d}\Delta\omega_i}{\mathrm{d}t} &= -\Delta P_i - D_i\ \Delta\omega_i, \end{aligned} \tag{9.84}$$

for $i \in \{\mathrm{G}\}$. As the network equations were derived in matrix form, it is convenient to write the above equation in matrix form too:

$$\begin{aligned} \Delta\dot{\boldsymbol{\delta}}_{\mathrm{G}} &= \Delta\boldsymbol{\omega}_{\mathrm{G}} \\ \boldsymbol{M}\Delta\dot{\boldsymbol{\omega}}_{\mathrm{G}} &= -\Delta\boldsymbol{P}_{\mathrm{G}} - \boldsymbol{D}\,\Delta\boldsymbol{\omega}_{\mathrm{G}}, \end{aligned} \tag{9.85}$$

where $\boldsymbol{M}$ and $\boldsymbol{D}$ are diagonal matrices of the inertia and damping coefficients, and $\Delta\boldsymbol{\delta}_{\mathrm{G}}$, $\Delta\boldsymbol{\omega}_{\mathrm{G}}$ and $\Delta\boldsymbol{P}_{\mathrm{G}}$ are column matrices of changes in rotor angles, rotor speed deviations and real power generations respectively.

Substituting (9.81) into the second equation of (9.85) gives the following state equation:

$$\boldsymbol{M}\,\Delta\dot{\boldsymbol{\omega}}_{\mathrm{G}} = -\boldsymbol{H}_{\mathrm{G}}\,\Delta\boldsymbol{\delta}_{\mathrm{G}} - \boldsymbol{D}\,\Delta\boldsymbol{\omega}_{\mathrm{G}} - \Delta\boldsymbol{K}_{\mathrm{ab}}\,h_{\mathrm{ab}}\,\Delta\gamma(t). \tag{9.86}$$

Here $\Delta\gamma(t)$ is the control function corresponding to the transformation ratio change of the phase shifting transformer. Function $\Delta\gamma(t)$ affects rotor motions in proportional to the coefficients $\Delta K_i h_{\mathrm{ab}} = (K_{i\mathrm{a}} - K_{i\mathrm{b}})h_{\mathrm{ab}}$.

The main question is how $\Delta\gamma(t)$ should be changed so that control of a given phase shifting transformer improves damping of oscillations. The control algorithm of $\Delta\gamma(t)$ will be derived using the Lyapunov direct method.

9.6.2 State-Variable Control Based on Lyapunov Method

In Section 6.3, the total system energy $V(\delta, \omega) = E_{\mathrm{k}} + E_{\mathrm{p}}$ was used as the Lyapunov function in the nonlinear system model (with line conductances neglected). In the considered linear model (9.86) the total system energy can be expressed as the sum of rotor speed and angle increments. This corresponds to expanding $V(\delta, \omega) = E_{\mathrm{k}} + E_{\mathrm{p}}$ in a Taylor series in the vicinity of an operating point, as in (6.11). This equation shows that $V(\boldsymbol{x})$ can be approximated in the vicinity of an operating point using a quadratic form based on the Hessian matrix of function $V(\boldsymbol{x})$.

For the potential energy E_{p} given by (6.47), the Hessian matrix corresponds to the gradient of real power generations and therefore also the Jacobi matrix used in the above incremental model:

$$\left[\frac{\partial^2 E_{\mathrm{p}}}{\partial\delta_i\partial\delta_j}\right] = \left[\frac{\partial P_i}{\partial\delta_j}\right] = \boldsymbol{H}_{\mathrm{G}}. \tag{9.87}$$

Equations (6.11) and (9.85) lead to

$$\Delta E_{\mathrm{p}} = \frac{1}{2}\Delta\boldsymbol{\delta}_{\mathrm{G}}^{\mathrm{T}}\boldsymbol{H}_{\mathrm{G}}\Delta\boldsymbol{\delta}_{\mathrm{G}} \tag{9.88}$$

It will be shown in Chapter 12 that if the network conductances are neglected, matrix $\boldsymbol{H}_{\mathrm{G}}$ is positive definite at an operating point (stable equilibrium point). Hence the quadratic form (9.88) is also positive definite.

Using (6.11), the kinetic energy E_{k} given by (6.46) can be expressed as

$$\Delta E_{\mathrm{k}} = \frac{1}{2}\Delta\boldsymbol{\omega}_{\mathrm{G}}^{\mathrm{T}}\boldsymbol{M}\,\Delta\boldsymbol{\omega}_{\mathrm{G}}. \tag{9.89}$$

This is a quadratic form made up of the vector of speed changes and a diagonal matrix of inertia coefficients. Matrix $\boldsymbol{M}$ is positive definite so the above quadratic form is also positive definite.

The total energy increment $\Delta V(\delta, \omega) = \Delta E_{\mathrm{k}} + \Delta E_{\mathrm{p}}$ is given by

$$\Delta V = \Delta E_{\mathrm{k}} + \Delta E_{\mathrm{p}} = \frac{1}{2}\Delta\boldsymbol{\omega}_{\mathrm{G}}^{\mathrm{T}}\,\boldsymbol{M}\,\Delta\boldsymbol{\omega}_{\mathrm{G}} + \frac{1}{2}\,\Delta\boldsymbol{\delta}_{\mathrm{G}}^{\mathrm{T}}\,\boldsymbol{H}_{\mathrm{G}}\Delta\boldsymbol{\delta}_{\mathrm{G}} \tag{9.90}$$

This function is positive definite as the sum of positive definite functions and therefore can be used as a Lyapunov function provided its time derivative at the operating point is negative definite.

Differentiating (9.88) and (9.89) gives

$$\Delta\dot{E}_{\mathrm{p}} = \frac{1}{2}\Delta\boldsymbol{\omega}_{\mathrm{G}}^{\mathrm{T}}\,\boldsymbol{H}_{\mathrm{G}}\Delta\boldsymbol{\delta}_{\mathrm{G}} + \frac{1}{2}\Delta\boldsymbol{\delta}_{\mathrm{G}}^{\mathrm{T}}\,\boldsymbol{H}_{\mathrm{G}}\Delta\boldsymbol{\omega}_{\mathrm{G}} \tag{9.91}$$

$$\Delta\dot{E}_{\mathrm{k}} = \frac{1}{2}\Delta\dot{\boldsymbol{\omega}}_{\mathrm{G}}^{\mathrm{T}}\boldsymbol{M}\Delta\boldsymbol{\omega}_{\mathrm{G}} + \frac{1}{2}\Delta\boldsymbol{\omega}_{\mathrm{G}}^{\mathrm{T}}\boldsymbol{M}\Delta\dot{\boldsymbol{\omega}}_{\mathrm{G}}. \tag{9.92}$$

Now, it is useful to transpose Equation (9.86):

$$\Delta\dot{\boldsymbol{\omega}}_{\mathrm{G}}^{\mathrm{T}}\,\mathbf{M} = -\Delta\delta_{\mathrm{G}}^{\mathrm{T}}\mathbf{H}_{\mathrm{G}} - \Delta\omega_{\mathrm{G}}^{\mathrm{T}}\mathbf{D} - \Delta\mathbf{K}_{\mathrm{ab}}^{\mathrm{T}}\,h_{\mathrm{ab}}\,\Delta\gamma(t). \tag{9.93}$$

Substituting the right hand side of (9.93) for $\Delta\dot{\boldsymbol{\omega}}_{\mathrm{G}}^{\mathrm{T}}\,\boldsymbol{M}$ in the first component of (9.92) gives

$$\begin{aligned}\Delta\dot{E}_{\mathrm{k}} = &-\frac{1}{2}\Delta\boldsymbol{\delta}_{\mathrm{G}}^{\mathrm{T}}\,\boldsymbol{H}_{\mathrm{G}}\,\Delta\boldsymbol{\omega}_{\mathrm{G}} - \frac{1}{2}\Delta\boldsymbol{\omega}_{\mathrm{G}}^{\mathrm{T}}\,\boldsymbol{H}_{\mathrm{G}}\,\Delta\boldsymbol{\delta}_{\mathrm{G}} - \Delta\boldsymbol{\omega}_{\mathrm{G}}^{\mathrm{T}}\,\boldsymbol{D}\,\Delta\boldsymbol{\omega}_{\mathrm{G}}\\ &-\frac{1}{2}\left(\Delta\boldsymbol{K}_{\mathrm{ab}}^{\mathrm{T}}\Delta\boldsymbol{\omega}_{\mathrm{G}} + \Delta\boldsymbol{\omega}_{\mathrm{G}}^{\mathrm{T}}\Delta\boldsymbol{K}_{\mathrm{ab}}\right)h_{\mathrm{ab}}\,\Delta\gamma(t).\end{aligned} \tag{9.94}$$

It can be easily checked that both expressions in the last component of (9.94) are identical scalars as

$$\Delta\boldsymbol{K}_{\mathrm{ab}}^{\mathrm{T}}\,\Delta\boldsymbol{\omega}_{\mathrm{G}} = \Delta\omega_{\mathrm{G}}^{\mathrm{T}}\,\Delta\boldsymbol{K}_{\mathrm{ab}} = \sum_{i\in\{\mathrm{G}\}}\Delta K_i\,\Delta\omega_i. \tag{9.95}$$

Hence Equation (9.94) can be rewritten as

$$\Delta\dot{E}_{\mathrm{k}} = -\frac{1}{2}\Delta\boldsymbol{\delta}_{\mathrm{G}}^{\mathrm{T}}\boldsymbol{H}_{\mathrm{G}}\Delta\boldsymbol{\omega}_{\mathrm{G}} - \frac{1}{2}\Delta\boldsymbol{\omega}_{\mathrm{G}}^{\mathrm{T}}\boldsymbol{H}_{\mathrm{G}}\Delta\boldsymbol{\delta}_{\mathrm{G}} - \Delta\boldsymbol{\omega}_{\mathrm{G}}^{\mathrm{T}}\boldsymbol{D}\Delta\boldsymbol{\omega}_{\mathrm{G}} - \Delta\boldsymbol{K}_{\mathrm{ab}}^{\mathrm{T}}\Delta\boldsymbol{\omega}_{\mathrm{G}}h_{\mathrm{ab}}\Delta\gamma(t). \tag{9.96}$$

Adding both sides of (9.96) and (9.91) gives

$$\Delta\dot{V} = \Delta\dot{E}_{\mathrm{k}} + \Delta\dot{E}_{\mathrm{p}} = -\Delta\boldsymbol{\omega}_{\mathrm{G}}^{\mathrm{T}}\boldsymbol{D}\Delta\boldsymbol{\omega}_{\mathrm{G}} - \Delta\boldsymbol{K}_{\mathrm{ab}}^{\mathrm{T}}\Delta\boldsymbol{\omega}_{\mathrm{G}}h_{\mathrm{ab}}\Delta\gamma(t). \tag{9.97}$$

In a particular case when there is no control, that is when $\Delta\gamma(t) = 0$, the equation in (9.97) gives

$$\Delta\dot{V} = \Delta\dot{E}_{\mathrm{k}} + \Delta\dot{E}_{\mathrm{p}} = -\Delta\boldsymbol{\omega}_{\mathrm{G}}^{\mathrm{T}}\boldsymbol{D}\Delta\boldsymbol{\omega}_{\mathrm{G}}. \tag{9.98}$$

As matrix $\boldsymbol{D}$ is positive definite, the function above is negative definite. Hence function (9.90) can be treated as the Lyapunov function for the system described by (9.86).

In order for the considered system to be stable when $\Delta\gamma(t) \neq 0$ changes, the second component in (9.97) should always be positive:

$$\Delta\boldsymbol{K}_{\mathrm{ab}}^{\mathrm{T}}\,\Delta\boldsymbol{\omega}_{\mathrm{G}}\,h_{\mathrm{ab}}\,\Delta\gamma(t) \geq 0. \tag{9.99}$$

This can be ensured using the following control law:

$$\Delta\gamma(t) = \kappa h_{\mathrm{ab}}\,\Delta\boldsymbol{K}_{\mathrm{ab}}^{\mathrm{T}}\,\Delta\boldsymbol{\omega}_{\mathrm{G}}. \tag{9.100}$$

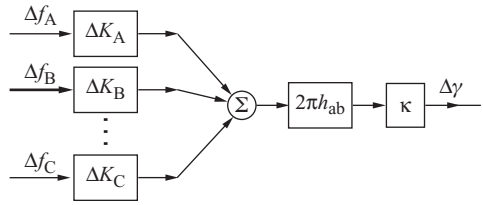

Figure 9.34 Block diagram of the stabilizing control loop of a power flow controller installed in a tie-line of an interconnected power system.

With this control law the derivative (9.97) of the Lyapunov function is given by

$$\Delta\dot{V} = -\Delta\boldsymbol{\omega}_G^T \boldsymbol{D}\Delta\boldsymbol{\omega}_G - \kappa\left(h_{ab}\Delta\boldsymbol{K}_{ab}^T\Delta\boldsymbol{\omega}_G\right)^2 \leq 0, \tag{9.101}$$

where κ is the control gain. Taking into account (9.95), the control law (9.100) can be written as

$$\Delta\gamma(t) = \kappa h_{ab} \sum_{i\in\{G\}} \Delta K_i \; \Delta\omega_i \tag{9.102}$$

where $\Delta K_i = K_{ia} - K_{ib}$ This control law is valid for any location of the phase shifting transformer. For the particular case when the phase shifting transformer is located in a tie-line, the control law can be simplified as described below.

The generator set $\{G\}$ in an interconnected system can be divided into a number of subsets corresponding to subsystems. Let us consider three subsystems as in Figure 9.34, that is $\{G\} = \{G_A\} + \{G_B\} + \{G_C\}$. Now the summation in Equation (9.102) can be divided into three sums:

$$\Delta\gamma(t) = \kappa h_{ab}\left[\sum_{i\in\{G_A\}} \Delta K_i \; \Delta\omega_i + \sum_{i\in\{G_B\}} \Delta K_i \; \Delta\omega_i + \sum_{i\in\{G_C\}} \Delta K_i \; \Delta\omega_i\right]. \tag{9.103}$$

Following a disturbance in one of the subsystems, there are *local swings* of generator rotors inside each subsystem and *interarea swings* of subsystems with respect to each other. The frequency of local swings is about 1 Hz while the frequency of interarea swings is much lower, usually about 0.25 Hz. Hence, when investigating the interarea swings, the local swings can be approximately neglected. Therefore it can be assumed that

$$\begin{aligned}
&\Delta\omega_1 \cong \cdots = \Delta\omega_i \cong \cdots \cong \Delta\omega_{n_A} \cong 2\pi\Delta f_A \quad \text{for} \quad i \in \{G_A\}\\
&\Delta\omega_1 \cong \cdots = \Delta\omega_i \cong \cdots \cong \Delta\omega_{n_B} \cong 2\pi\Delta f_B \quad \text{for} \quad i \in \{G_B\}\\
&\Delta\omega_1 \cong \cdots = \Delta\omega_i \cong \cdots \cong \Delta\omega_{n_C} \cong 2\pi\Delta f_C \quad \text{for} \quad i \in \{G_C\}.
\end{aligned} \tag{9.104}$$

Now Equation (9.103) can be expressed as

$$\Delta\gamma(t) = \kappa 2\pi h_{ab}\left[\Delta f_A \sum_{i\in\{G_A\}} \Delta K_i + \Delta f_B \sum_{i\in\{G_B\}} \Delta K_i + \Delta f_C \sum_{i\in\{G_C\}} \Delta K_i\right], \tag{9.105}$$

or, after summing the coefficients,

$$\Delta\gamma(t) = \kappa 2\pi h_{ab}\left(\Delta K_A \; \Delta f_A + \Delta K_B \; \Delta f_B + \Delta K_C \; \Delta f_C\right), \tag{9.106}$$

where

$$\Delta K_{\mathrm{A}} = \sum_{i \in \{\mathrm{G_A}\}} \Delta K_i, \quad \Delta K_{\mathrm{B}} = \sum_{i \in \{\mathrm{G_B}\}} \Delta K_i, \quad \Delta K_{\mathrm{C}} = \sum_{i \in \{\mathrm{G_C}\}} \Delta K_i. \tag{9.107}$$

Equation (9.106) shows that the control of a phase shifting transformer should employ the signals of frequency deviations weighted by coefficients (9.107).

A block diagram of the supplementary control loop based on (9.106) is shown in Figure 9.34. The way in which the supplementary control loop is added to the overall regulator was shown earlier in Figure 9.31.

The input signals to the supplementary control are frequency deviations Δf in each subsystem. These signals should be transmitted to the regulator using telecommunication links or WAMS discussed in Section 2.6. For the frequency of interarea swings of about 0.25 Hz, the period of oscillation is about 4 s and the speed of signal transmission to the regulator does not have to be high. It is enough if the signals are transmitted every 0.1 s, which is not a tall order for modern telecom systems.

The coefficients h_{ab}, ΔK_{A} , ΔK_{B} , ΔK_{C} in (9.106) have to be calculated by an appropriate SCADA/EMS function using current state estimation results and the system configuration. Obviously those calculations do not have to be repeated frequently. Modifications have to be done only after system configuration changes or after a significant change of power system loading.

When deriving Equation (9.106), for simplicity only one phase shifting transformer was assumed. Similar considerations can be taken for any number of phase shifting transformers installed in any number of tie-lines. For each transformer, identical control laws are obtained but obviously with different coefficients calculated for the respective tie-lines.

9.6.3 Example of Simulation Results

Neglecting local swings within the subsystems of an interconnected system, Equations (9.104), a simplified system model can be created using the incremental network model. This model, described by Rasolomampionona (2007), can take into account frequency and tie-line control and include models of phase shifting transformers installed in tie-lines. An example of the influence of phase shifting transformer regulation will be described below using simulation results.

Figure 9.35 shows a test system with parameters. All three tie-lines contain TCPAR-type devices controlled by the regulators shown in Figure 9.34. The stabilizing controllers use frequency deviations as their input signals.

Figure 9.36 shows the simulation results for a power balance disturbance $\Delta P_0 = 200$ MW consisting of an outage of a generating unit in system A. A thick line shows the responses when a TCPAR device was active and a thin line the responses when the device was not active. Frequency changes in the subsystems are shown in Figure 9.36a. When TCPAR devices are not active, frequency responses are affected by interarea oscillations (the thin line). Active TCPAR devices quickly damp out the interarea oscillations and the remaining slow frequency changes are due to the frequency and tie-line flow control (the thick line). The maximum frequency deviation in subsystems B and C is reduced due to the action of the TCPAR.

Tie-line flow changes are shown in Figure 9.36b. When TCPAR devices are not acting, changes due to frequency and tie-line flow control are superimposed on interarea swings (the thin line). Acting TCPAR devices quickly damp out the interarea swings. The remaining tie-line deviations tend to zero with time, which shows that the non-intervention rule is fulfilled. Fulfilment of the rule is also visible in Figure 9.36b showing generation changes. Following the power balance disturbance in subsystem A, subsystems B and C support A for a short time by means of a power injection. As the frequency returns to its reference value and subsystem A increases its generation, generation

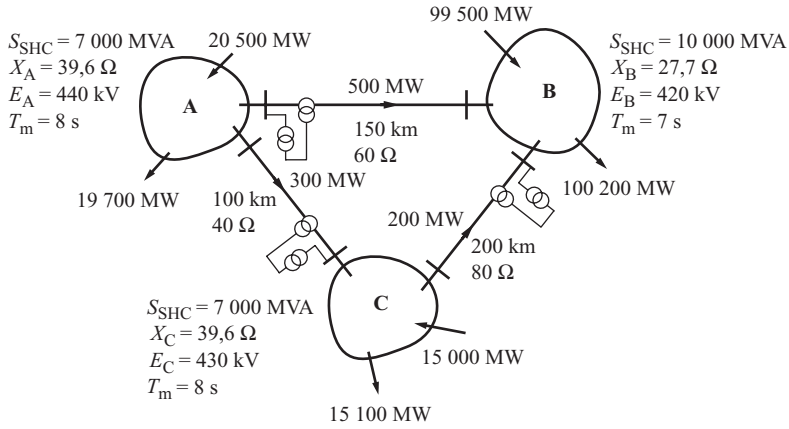

Figure 9.35 A test system.

in B and C returns to its initial value. The diagram also shows interarea oscillations in generation (especially in subsystem C) when the TCPAR device was not active.

9.6.4 Coordination Between AGC and Series FACTS Devices in Tie-Lines

The power flow controller shown in Figure 9.31 can be treated as a multi-level controller consisting of three control paths:

level 1: supplementary control loop with frequency deviations Δf_A , Δf_B , Δf_C as the input signals (Figure 9.34);
level 2: main control path with real power P_{tie} as the input signal;
level 3: supervisory control at SCADA/EMS level setting $P_{tie\ ref}$.

The actions of these three control loops are superimposed on top of each other and, through changes in $\gamma(t)$, influence tie-line flows and therefore also operation of AGC in individual subsystems of an interconnected power system. In order for both FACTS and AGC controls to be effective and beneficial for the power system, there must be appropriate coordination. This coordination has to be achieved by adjusting the speed of operation of the three control paths of the FACTS devices to the speed of operation of the three levels of AGC (primary, secondary, tertiary). The three control loops of AGC (Figure 9.12) differ widely in their speed of operation. The three control levels of the FACTS device installed in the tie-line of an interconnected power system must also exhibit a similarly differing speed of operation.

Referring to the description of four stages of power system dynamics due to AGC after a large power imbalance (Sections 9.2–9.5) and the description of operation of a TCPAR-type FACTS device (Section 9.6.4), the following conclusions can be drawn about time coordination of individual control levels.

Supplementary loop control (level 1) should respond quickly, according to the control law (9.106), to frequency changes due to interarea swings. Hence the speed of reaction of that control level must be the fastest, similar to that of primary control performed by AGC (prime mover control).

Control executed in the main path (level 2) cannot be fast and must be slower than secondary control performed by AGC (frequency and tie-line flow control). This can be explained in the

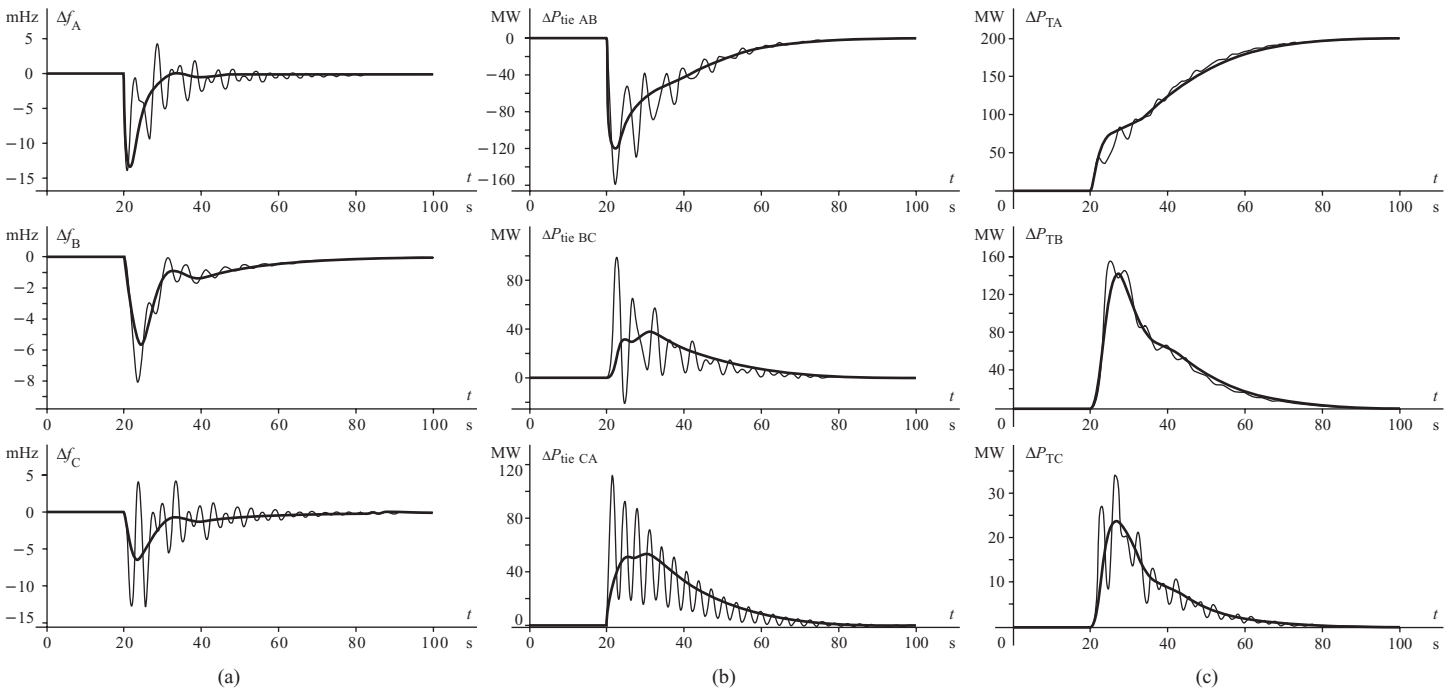

Figure 9.36 Simulation results following a power balance disturbance in subsystem A: (a) local frequency changes; (b) tie-line flow changes; (c) generation changes.

following way. Following a real power imbalance in a given subsystem, a power injection, lasting several tens of seconds, may flow to that subsystem from the other subsystems (Figure 9.36b). This power injection causes P_{tie} to be different from $P_{\text{tie ref}}$ and a control error appears in that control path. If the controller reacted too quickly, then the FACTS device could affect the power injection which would adversely affect the frequency control of the secondary level of AGC. The maximum frequency deviation would increase and the quality of regulation would decrease (Figure 9.13). To prevent this, the discussed control level should act with a long time constant. Figure 9.31 shows that the main control path contains an integrator with a feedback loop. The transfer function of the element is $G(\text{s}) = 1/(\rho_{\text{P}} + T_{\text{P}}\text{s})$, which means that the speed of operation of the element is determined by the time constant $T_{\text{P}}/\rho_{\text{P}}$ If this time constant is several times higher than the duration time of power injection then the discussed control level should not adversely affect secondary control executed by AGC.

The supervisory control (level 3) setting $P_{\text{tie ref}}$ executed by SCADA/EMS must be the slowest. Especially important for the dynamic performance is the case shown in Figure 9.36d when insufficient regulation power in the subsystem where the power imbalance occurred must result in a permanent deviation in exchanged power. The FACTS device controlled by the regulator shown in Figure 9.31 will try to regulate P_{tie} to a value $P_{\text{tie ref}}$ It may turn out that such regulation is not beneficial for the system and result in, for example, overloading of other transmission lines. Regulation at that level must be centrally executed by SCADA/EMS based on the analysis of the whole network.